Marine Life Science & Technology
https://doi.org/10.1007/s42995-025-00320-x

RESEARCH PAPER

Isochrysis zhanjiangensis exhibits protective effects against metabolic abnormalities induced by high-fat diet in mice

Mei Wu[1] · Yu Bai[1] · Yanrong Li[2] · Kang Chen[1] · Jingyang Le[3] · Jian Li[4] · Chengxu Zhou[1] · Spiros N. Agathos[4,5] · Lin Zhang[6] · Xiaojun Yan[7] · Jichang Han[1]

Received: 23 December 2024 / Accepted: 11 August 2025
© Ocean University of China 2025

Abstract

While *Isochrysis zhanjiangensis*, a marine microalga, has been widely adopted in aquaculture for its health-promoting properties, its potential as a functional food for human metabolic health remains unexplored. To bridge this gap, this study systematically evaluated the nutritional composition, biosafety, and therapeutic efficacy of *I. zhanjiangensis* against high-fat diet (HFD)-induced metabolic disorders in mice. Our results revealed that *I. zhanjiangensis* exhibits a desirable nutritional profile with no detectable toxicity, and its dietary supplementation significantly attenuated HFD-induced metabolic dysregulation. Gut microbiota profiling further demonstrated that *I. zhanjiangensis* supplementation restored microbial homeostasis, evidenced by mitigation of the elevated Firmicutes/Bacteroidota ratio and enrichment of beneficial genera including *Muribaculum*, *Candidatus_Arthromitus*, and *Veillonella*. Hepatic metabolomics identified key metabolites modulated by *I. zhanjiangensis*, such as N1-methyl-2-pyridone-5-carboxamide, N-acetyl-L-histidine, and eicosapentaenoic acid, which are mechanistically linked to lipid metabolism regulation. These findings not only position *I. zhanjiangensis* as a promising candidate for functional food development targeting HFD-induced metabolic dysregulation, but also highlight the untapped potential of aquaculture microalgae as sustainable resources for nutraceutical innovation.

Keywords Bait microalgae · High-fat diet · *Isochrysis zhanjiangensis* · Microbiota stability · Metabolomics

Introduction

The global transition towards industrialized diets, predominantly high-fat diets (HFDs), has escalated the incidence of metabolic disorders, including hyperlipidemia, obesity, type 2 diabetes, and cardiovascular diseases (CVDs) (Cheng et al. 2023). Mechanistically, prolonged HFD intake drives these pathologies by inducing systemic metabolic dysregulation, characterized by insulin resistance, ectopic lipid accumulation in non-adipose tissues (like the liver), chronic low-grade inflammation, and potentially detrimental shifts in gut microbiota composition (Sakamoto et al. 2025). Current therapeutic strategies often rely on pharmacological interventions targeting, for instance, dyslipidemia or hyperglycemia, which can provide significant symptomatic relief (Magni et al. 2015). However, concerns regarding long-term efficacy, patient compliance, potential side effects (such as gastrointestinal issues or muscle pain with statins), and the inability to fully reverse underlying pathologies drive the search for complementary and alternative strategies. Notably, preventative and adjunctive approaches focusing

Edited by Xin Yu.

✉ Jichang Han
Hanjichang@nbu.edu.cn

1 College of Food Science and Engineering, Ningbo University, Ningbo 315211, China

2 Ningbo Institute of Oceanography, Ningbo 315832, China

3 School of Medicine, Ningbo University, Ningbo 315211, China

4 Qingdao Innovation and Development Base, Harbin Engineering University, Qingdao 266000, China

5 Earth and Life Institute, Bioengineering Laboratory, Catholic University of Louvain, 1348 Louvain-La-Neuve, Belgium

6 Key Laboratory of Applied Marine Biotechnology, Ministry of Education of China, Ningbo University, Ningbo 315832, China

7 Collaborative Innovation Center for Zhejiang Marine High-Efficiency and Healthy Aquaculture, Ningbo University, Ningbo 315211, China

Published online: 01 October 2025

on bioactive compounds from natural sources, particularly functional foods, have emerged as promising avenues for mitigating HFD-induced metabolic disorders, often with potentially favorable safety profiles compared to long-term medication use (Nayak et al. 2021).

Microalgae, phylogenetically diverse photosynthetic microorganisms underpinning aquatic ecosystems, are recognized as sustainable reservoirs of nutraceuticals, including polyunsaturated fatty acids (PUFAs) and carotenoids with evidenced bioactivities (Matos et al. 2017). Among them, certain genera (*e.g.*, *Chaetoceros*, *Phaeodactylum*, *Nannochloropsis*, and *Tetraselmis*) extensively used in aquaculture, termed bait microalgae, have a long history of enhancing the growth and health of farmed marine organisms, attesting to their nutritional value and toxicological safety within that context (Atalah et al. 2007; Vizcaíno et al. 2016). Moreover, the safety of these microalgae has been rigorously evaluated by food safety authorities such as the U.S. Food and Drug Administration (FDA) and the European Food Safety Authority (EFSA), confirming their biosafety for industrial aquafeed formulations (Shah et al. 2018). Paradoxically, despite their proven biosafety, high nutritional properties, and large-scale cultivation, their translational potential as functional ingredients for mitigating human metabolic disorders or enhancing human health remains largely underexplored (Ma et al. 2020a).

Isochrysis zhanjiangensis, a marine chrysophyte, is a high-value microalga widely employed in mariculture due to its exceptional nutritional profile, particularly its high content of PUFAs such as eicosapentaenoic acid (EPA) and docosahexaenoic acid (DHA) (Mohammad and Wan 2017). The biomass further contains bioactive metabolites with demonstrated metabolic benefits, including the carotenoid fucoxanthin and polyphenols known for their ability to counteract key features of HFD-induced metabolic dysregulation, such as inflammation, obesity, and hyperlipidemia (Yang et al. 2023a). Notably, while studies on isolated components (*e.g.*, peptides with cardiovascular protective effects) (Chen et al. 2019) or ethanol extracts mitigating alcohol-induced hepatotoxicity (Wen et al. 2024) have provided mechanistic insights, they overlook the food matrix effect (Liu et al. 2024a; Qian et al. 2021). This phenomenon, where the bioactivity of whole foods exceeds the sum of isolated constituents due to component synergy (Jacobs and Tapsell 2007), remains unexplored for *I. zhanjiangensis*. Specifically, the potential of its whole biomass to counteract HFD-induced metabolic disorders through multi-target interactions within a complex dietary context warrants systematic investigation.

Given the established role of the gut-liver axis in metabolic health (Tilg et al. 2022) and the documented modulatory effects of dietary PUFAs and fucoxanthin on both gut microbiota composition and hepatic lipid metabolism (Schoeler et al. 2023; Zhou et al. 2025), we hypothesized that the whole biomass of *I. zhanjiangensis*, rich in these bioactive components, could ameliorate HFD-induced metabolic dysregulation via synergistic interactions with host-microbiota crosstalk. To test this hypothesis, the present study aimed to: comprehensively characterize the nutritional profile of *I. zhanjiangensis*; rigorously evaluate its biosafety through acute (14 days) and chronic (10 weeks) toxicity studies in mice, including histopathological and serum biochemical analyses; quantify its therapeutic efficacy against HFD-induced metabolic perturbations, including adiposity, hepatic steatosis, and systemic inflammation; decipher underlying mechanisms by integrating multi-omics analyses, including 16S rRNA sequencing for gut microbiota diversity and untargeted metabolomics for hepatic metabolic pathway profiling. The findings are expected to validate *I. zhanjiangensis* as a novel, safe, and multifunctional dietary intervention for metabolic syndrome, further advancing the utilization of aquaculture-proven microalgae as sustainable nutraceutical resources.

Materials and methods

Nutritional composition analysis

The lyophilized *I. zhanjiangensis* powder, artificially cultivated in indoor photobioreactors, was provided by SDIC Microalgae Biotechnology Center, SDIC Biotechnology Investment Co. Ltd., Beijing, China. Total lipid content was determined using the chloroform–methanol ($CHCl_3$-CH_3OH) extraction method, protein content was measured using the Coomassie Brilliant Blue G250 assay, and carbohydrate content was assessed using the Phenol–Sulfuric Acid method. The ash content was quantified by weight difference. All parameters were determined based on three independent biological replicates of the lyophilized powder to ensure reproducibility. Fatty acids (FAs) were analyzed using gas chromatography-mass spectrometry (GC–MS). Lipid nutritional indices, including the atherogenicity index (AI), hypocholesterolemic/hypercholesterolemic ratio (HH), thrombogenicity index (TI), and PUFA/SFA ratio, were calculated based on the FAs profile. Pigments were detected using ultra-high-performance liquid chromatography (UHPLC), and free amino acids (FAAs) were quantified using an automatic amino acid analyzer. Volatile organic compounds (VOCs) were determined using an Agilent 7890B-7000C GC system. All details related to this section are shown in Supplementary Appendix A (Methods S1).

Acute and chronic toxicity and safety assessment in mice

Six-week-old male C57BL/6 mice (weighing 19.57 ± 0.48 g) were purchased from the Animal Center of Zhejiang

Academy of Medical Sciences (Hangzhou, China). The study protocol was approved by the Animal Care and Use Committee of Ningbo University (Approval No. NBU20220102, dated 2022), and all animal experiments were conducted in compliance with the National Institutes of Health (NIH) Guide for the Care and Use of Laboratory Animals (NIH Publications No. 80–23, revised 1996).

In the acute toxicity limit dose test, mice were administered a single dose of *I. zhanjiangensis* (lyophilized powder suspended in saline) (5000 mg/kg BW) via oral gavage and were observed for two weeks for any signs of toxicity. In the 10 weeks chronic feeding test, thirty mice were randomly divided into three groups ($n = 10$ per group) and fed according to a specific regimen for the duration of the study. One group (*Isochrysis* Low-dose, IL) received *I. zhanjiangensis* via oral gavage at a dosage of 200 $mg \cdot kg^{-1} \cdot d^{-1}$, another group (*Isochrysis* High-dose, IH) received *I. zhanjiangensis* via oral gavage at a dosage of 400 $mg \cdot kg^{-1} \cdot d^{-1}$. The control group (Con) received an equivalent volume of saline solution via oral gavage as the vehicle control (Chamorro-Cevallos et al. 2008; Li et al. 2020). Throughout the feeding period, mice were monitored daily for general health status, including fur condition, behavior, and signs of distress. Feed and water intake were measured daily, and BW was recorded weekly. At the end of the chronic feeding trials, blood samples were collected, and serum was separated for biochemical analysis. Serum indices, including liver function enzymes and lipid profiles, were analyzed using commercial kits. Following both the acute and chronic feeding trials, mice were euthanized, and liver and kidney were harvested, rinsed, fixed in a 4% paraformaldehyde solution, and then stained with Hematoxylin and Eosin (H&E) for further analysis. Histological examinations were conducted using a Nikon Eclipse Ci-E microscope (Nikon Instruments Inc., Japan). Detailed methodology is provided in Supplementary Appendix A (Methods S2).

Evaluation of protective effects of *I. zhanjiangensis* on HFD-induced metabolic disorders in mice

Forty six weeks-old male C57BL/6 mice (weighing 19.25 ± 0.33 g) were randomly assigned to four groups ($n = 10$ per group): normal diet (ND) group receiving standard chow (15.8 kcal% fat, Diet 10293G), HFD group receiving a high-fat diet (60 kcal% fat diet, Diet D12492), HFD supplemented with 200 $mg \cdot kg^{-1} \cdot d^{-1}$ of *I. zhanjiangensis* (HFDIL), and HFD supplemented with 400 $mg \cdot kg^{-1} \cdot d^{-1}$ of *I. zhanjiangensis* (HFDIH). During the 10 weeks feeding period, food intake was recorded daily, from which daily energy intake was calculated, and BW was measured weekly. At the end of the feeding period, mice were euthanized, and blood samples were collected for serum biochemical analysis. White adipose tissue (WAT) and liver weights were measured. Liver tissues were processed for histological analysis using both H&E staining and Oil Red O staining to assess steatosis, while kidney tissues were analyzed using H&E staining. Serum biochemical parameters, including liver enzymes, lipid profiles, and inflammatory markers, were analyzed using commercial kits. The compositions of ND and HFD diet are shown in Supplementary Table A.1, and detailed methodology related to this section is provided in Supplementary Appendix A (Methods S3).

Analysis of gut microbiota composition and liver metabolomic profiles

At the end of the feeding trials, approximately 50 mg of liver tissue from each mouse was harvested, flash-frozen in liquid nitrogen, and stored at − 80 °C for metabolomic analysis using LC–MS/MS. Fecal samples were collected from six mice per group, and microbial DNA was extracted using the QIAamp Fast DNA Stool Mini Kit (Qiagen, Germany) according to the manufacturer's instructions. The V3–V4 region of the 16S rRNA gene was amplified using the primers 314F and 806R, and sequencing was performed on the Illumina MiSeq platform (Illumina, USA) at Beijing Novogene Technology Co., Ltd. Details regarding gut microbiota and liver metabolomics analysis are shown in Supplementary Appendix A (Methods S4).

Statistical analysis

All parameters were tested with three biological replicates per treatment, and the results were presented as the mean ± standard deviation (SD). Significant differences between two groups were determined using the *T*-test, while differences among multiple groups were assessed using one-way ANOVA followed by Tukey's HSD post-hoc test. The online Venn diagram tool (http://www.ehbio.com/test/venn/#/) was used for data visualization and interpretation. Spearman correlation coefficients between biochemical indicators, gut microbiota, and metabolites were evaluated using R v4.2.1.

Results

Nutritional properties

In this study, the nutritional properties of *I. zhanjiangensis* were systematically characterized by analyzing the macronutrients (lipids, proteins, carbohydrates, and ash) and bioactive compounds (FAs, pigments, and FAAs). Key nutritional indices, such as the ω6/ω3 ratio, PUFA/SFA ratio, AI, TI, and HH ratio were evaluated to assess health implications. Moreover, the VOC profile was assessed to investigate

their potential contribution to flavor characteristics in food applications.

In terms of macronutrients, *I. zhanjiangensis* exhibited a high lipid content of 35.9% and a moderate protein content of 26.0% (Fig. 1A). The carbohydrate content was relatively low at 8.3%, suggesting a potential preference for lipids over carbohydrates as primary energy reserves. Furthermore, the absence of a rigid cell wall resulted in a significantly lower ash content compared to other microalgae such as *Tetraselmis suecica*, *Phaeodactylum tricornutum*, and *Chlorella vulgaris* (Batista et al. 2019).

Analysis of the FA profile identified 13 types of FAs in *I. zhanjiangensis*. PUFAs were the most abundant, comprising 45.06% of the total FA, followed by SFAs (32.79%) and monounsaturated fatty acids (MUFAs, 22.15%) (Fig. 1B) (Supplementary Appendix B, Fig. cB.1). Among PUFAs, the ω3 type—including DHA (22:6 ω3) and α-linolenic acid (ALA, 18:3 ω3)—was significantly higher than the ω6 type, resulting in a low ω6/ω3 ratio of approximately 0.25. Key nutritional indices, including the PUFA/SFA ratio, AI, TI, and HH ratio, were calculated to evaluate lipid quality, yielding values of 1.38, 1.06, 0.21, and 2.11, respectively (Fig. 1C).

I. zhanjiangensis contained significant levels of pigments, including chlorophyll a (58.1 mg/g) and total carotenoids (23.0 mg/g), as shown in Fig. 1D (Supplementary Appendix B, Fig. B.2). Fucoxanthin (15.6 mg/g), a major carotenoid, accounted for approximately two-thirds of the total carotenoid content.

In total, 21 FAAs were identified in *I. zhanjiangensis*, with concentrations ranging from 33.16 μg/g (5-hydroxylysine) to 1348.49 μg/g (alanine). Both essential amino acids (EAAs) and non-essential amino acids (NEAAs) were present, with EAA/(EAA + NEAA) and EAA/NEAA ratios calculated at 35% and 54%, respectively (Fig. 1E). Notably, taste-active amino acids, including lysine, alanine, valine, and arginine, were identified as key flavor contributors to its profile, supported by their taste activity values (TAVs) exceeding 1 (Supplementary Appendix B, Table B.1) (Zheng et al. 2015).

VOC analysis revealed a complex profile comprising 26 distinct compounds categorized into ten chemical classes (Fig. 1F) (Supplementary Appendix B, Fig. B.3 and Table B.2). Acids, sulfur-containing compounds, and halohydrocarbons dominated the profile, collectively contributing to the characteristic aroma of *I. zhanjiangensis*. Key odor-active VOCs included 2-propenoic acid (pungent/acidic note), chloroethene (ethereal odor), and dimethyl sulfoxonium formylmethylidene (sulfurous aroma).

Safety assessment

The safety of *I. zhanjiangensis* was evaluated through acute toxicity and chronic feeding studies. In the acute toxicity test, mice administered a single oral limit dose of 5000 mg/kg BW exhibited no mortality or adverse clinical signs during the 14 days observation period. BWs remained consistent across all groups, ranging from 25.00 to 28.90 g, with no statistically significant differences (Supplementary Appendix B, Fig. B.4A). Furthermore, histopathological examination of liver and kidney tissues collected at the end of the observation period revealed no treatment-related microscopic abnormalities (Supplementary Appendix B, Fig. B.4B).

In the 10 weeks feeding study, no abnormalities were observed in general health parameters, including fur condition, ocular morphology, and locomotor activity. BWs, daily food intake, and water consumption showed no intergroup differences (Fig. 2A–C). Serum biochemical analysis revealed significant metabolic benefits in the IH group (400 $mg \cdot kg^{-1} \cdot d^{-1}$) compared to the Con group. Specifically, IH mice showed significantly lower blood glucose (BG; 4.53 vs. 5.04 mmol/L) and uric acid (UA; 34.82 vs. 37.85 μmol/L), coupled with higher high-density lipoprotein cholesterol (HDL-C; 2.56 vs. 2.29 mmol/L) (Fig. 2D–F). In contrast, no significant differences were found among the groups for other key parameters such as total cholesterol (TC), triglycerides (TG), low-density lipoprotein cholesterol (LDL-C), liver enzymes (aspartate aminotransferase, AST; alanine aminotransferase, ALT), and creatinine (CRE). Representative values for these non-significant markers included TC ranging from 2.05 (IH) to 2.27 (Con) mmol/L, TG from 0.79 (IH) to 0.99 (Con) mmol/L, LDL-C from 0.66 (IH) to 0.72 (Con) mmol/L, AST from 24.83 (Con) to 26.26 (IL, 200 $mg \cdot kg^{-1} \cdot d^{-1}$) U/L, ALT from 18.90 (IL) to 19.45 (Con) U/L, and CRE from 34.82 (IH) to 39.19 (Con) μmol/L. Histological examination of liver tissue (Fig. 2G) revealed preserved hepatic architecture across all groups, characterized by well-defined hepatic plates, hepatic sinusoids, and identifiable Kupffer cells. No evidence of inflammatory infiltration, steatosis, or necrosis was observed. Similarly, kidney tissue sections (Fig. 2H) demonstrated normal morphology, with structurally intact renal corpuscles, proximal tubules, and distal tubules. The tubular epithelial cells maintained their integrity, and there were no discernible signs of degeneration, cast formation, or interstitial fibrosis.

Effects of *I. zhanjiangensis* on alleviating HFD-induced metabolic disorders

To evaluate the protective effects of *I. zhanjiangensis* against HFD-induced metabolic disorders, mice were fed an HFD with or without *I. zhanjiangensis* supplementation for 10 weeks. Compared to the ND group (8.33 g), HFD-fed

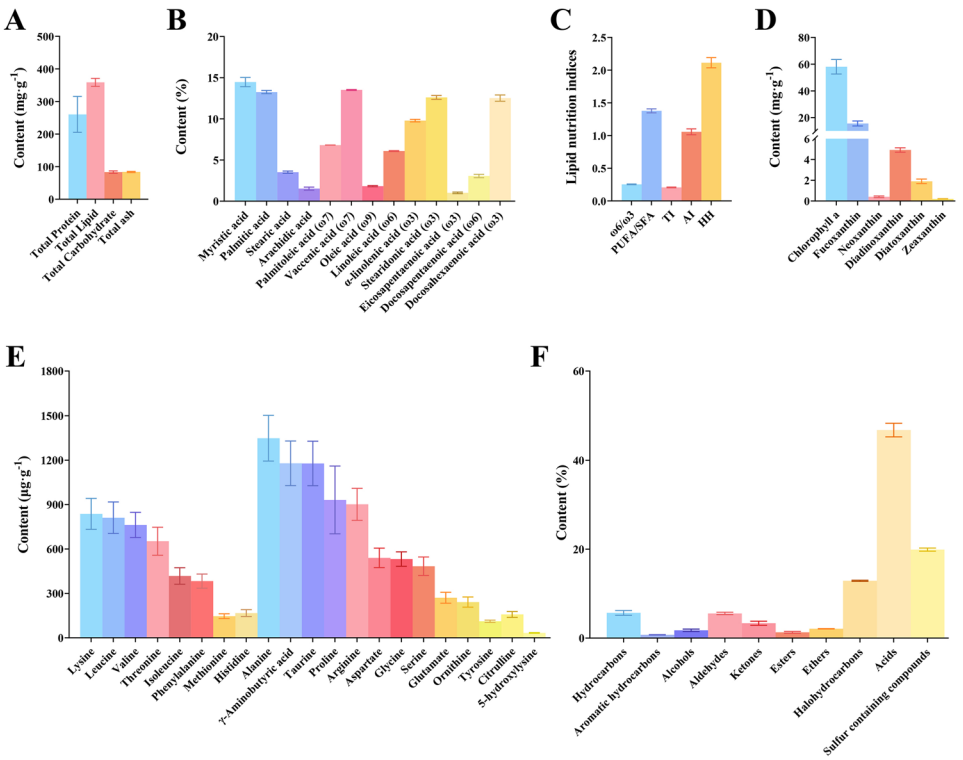

Fig. 1 Nutritional profile of *Isochrysis zhanjiangensis*. **A** Macronutrient compositions. **B** FA profile. **C** Lipid nutritional indices. **D** Pigments. **E** FAA profile. **F** VOC profile. ω6/ω3, PUFA/SFA, HH, TI, and AI in **C** represent the ω6 to ω3 unsaturated fatty acid ratio, polyunsaturated fatty acid to saturated fatty acid ratio, hypocholesterolemic/hypercholesterolemic ratio, thrombogenicity index, and atherogenicity index, respectively

mice exhibited a significant increase in BW gain (17.38 g) (Fig. 3A, B). However, supplementation with *I. zhanjiangensis* dose-dependently attenuated this effect, reducing BW gain to levels comparable to the ND group in the HFDIH group (8.00 g), with no significant difference observed between these two groups.

HFD-induced increases in both WAT mass (1.93 g) and liver weight (1.23 g), key indicators of ectopic lipid accumulation, were significantly reduced by *I. zhanjiangensis* supplementation in the HFDIL (0.92 and 0.88 g for WAT mass and liver weight, respectively) and HFDIH (0.69 and 0.74 g for WAT mass and liver weight, respectively) groups (Fig. 3C). Notably, despite comparable energy intake across all groups (Fig. 3D), the reduced BW gain in supplemented groups suggested that the anti-obesity effects of *I. zhanjiangensis* were likely mediated by enhancing metabolic homeostasis rather than suppressing appetite.

Histological examination using H&E and Oil Red O staining revealed intact hepatic architecture with no lipid droplets in the ND group (Fig. 3E). In contrast, HFD-fed mice exhibited severe hepatic steatosis characterized by extensive lipid droplet deposition (Fig. 3F), accompanied by signs of hepatocellular damage, disorganized lobular structure, and mild inflammatory cell infiltration. Dietary supplementation with *I. zhanjiangensis* significantly ameliorated these alterations, particularly reducing lipid droplet area by 99% (HFDIH) compared to the HFD group.

Serum biochemical analysis revealed pronounced hepatic injury in the HFD group, with elevated ALT (from 20.05 U/L to 56.12 U/L) and AST (from 28.39 U/L to 95.29 U/L) levels compared to the ND group. *I. zhanjiangensis* supplementation significantly reduced these levels in the HFDIL (45.47 U/L and 77.09 U/L for ALT and AST, respectively) and HFDIH (42.12 U/L and 67.43 U/L for ALT and AST, respectively) groups (Fig. 3G). Furthermore, lipid profile analysis demonstrated that the HFD group exhibited dyslipidemia, with significant increases in TC, TG, and LDL-C, and a decrease in HDL-C (Fig. 3H). *I. zhanjiangensis* supplementation restored lipid homeostasis, particularly in the HFDIH group, where TG and TC levels were normalized to ND levels.

Furthermore, the HFD group exhibited a significant pro-inflammatory profile compared to the ND group, characterized by elevated levels of lipopolysaccharide (LPS; 7.18 vs. 4.69 U/L), tumor necrosis factor-alpha (TNF-α; 17.65 vs. 11.10 pg/mL), and interleukin-6 (IL-6; 35.04 vs. 22.27 pg/mL), alongside reduced levels of the anti-inflammatory cytokine interleukin-10 (IL-10; 66.90 vs. 100.86 pg/mL) (Fig. 3I, J). *I. zhanjiangensis* supplementation dose-dependently reversed this imbalance. The HFDIL group showed significant improvements (LPS: 6.34 U/L; TNF-α: 12.81 pg/mL; IL-6: 31.22 pg/mL; IL-10: 72.38 pg/mL), while the HFDIH group exhibited levels restored to near-normal (LPS: 5.28 U/L; TNF-α: 11.23 pg/mL; IL-6: 28.98 pg/mL; IL-10: 78.74 pg/mL).

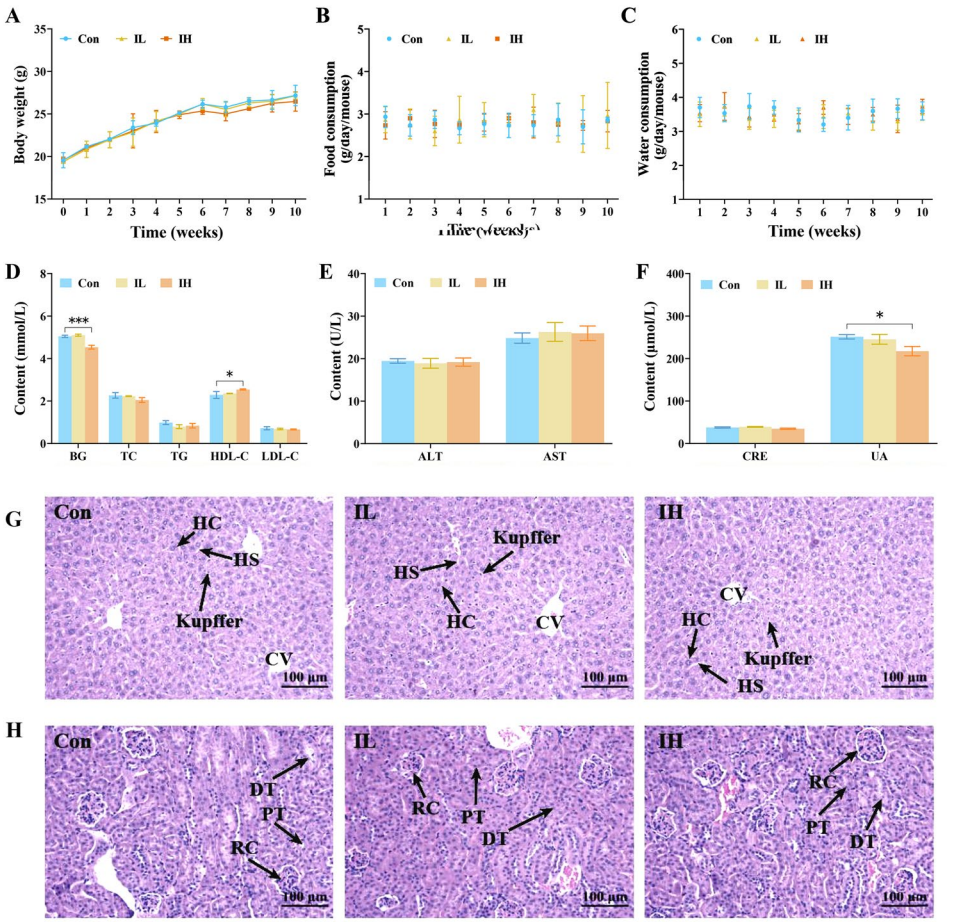

Fig. 2 Chronic toxicity assessment of *Isochrysis zhanjiangensis*. **A** Body weight. **B** Food consumption. **C** Water consumption. **D** Serum indices of blood glucose (BG), total cholesterol (TC), triglycerides (TG), high-density lipoprotein cholesterol (HDL-C), and low-density lipoprotein cholesterol (LDL-C). **E** Serum indices of alanine aminotransferase (ALT) and aspartate aminotransferase (AST). **F** Serum indices of creatinine (CRE) and uric acid (UA). **G**, **H** H&E-stained sections of liver and kidney tissues; CV: central vein; HC: hepatic cell; HS: hepatic sinusoid; Kupffer: Kupffer cell; RC: renal corpuscle; PT: proximal tubule; DT: distal tubules. $^{*}P < 0.05$, $^{***}P < 0.001$

Effects of *I. zhanjiangensis* on the liver metabolic profile

Untargeted metabolomics analysis of liver tissues using LC–MS/MS revealed that supplementation with *I. zhanjiangensis* partially ameliorated HFD-induced systemic metabolic perturbations. Principal component analysis (PCA) and orthogonal partial least squares-discriminant analysis (OPLS-DA) models demonstrated distinct clustering among ND, HFD, and HFDIH groups (Fig. 4A, B). The HFDIH group exhibited intermediate metabolic profiles between ND and HFD clusters, particularly in the restoration of key metabolites including EPA and bile acids, suggesting a restorative effect of *I. zhanjiangensis*. S-plots derived from OPLS-DA identified 38 metabolites that contributed significantly to group separations, with model validity confirmed by robust parameters ($R^2X = 0.776$–0.849, $Q^2 = 0.624$–0.664 for positive and negative ion modes, respectively) (Supplementary Appendix B, Fig. B.5).

Comparative analysis revealed significant alterations in 28 metabolites induced by HFD (ND vs. HFD), demonstrating multi-faceted metabolic dysregulation. The most prominent changes included a marked depletion of anti-inflammatory EPA (65% decrease) accompanied by disrupted bile acid homeostasis, evidenced by substantial reductions in both conjugated taurocholic acid (60% decrease) and primary cholic acid (17% decrease). Changes related to oxidative stress pathways included a significant decrease in the plant-derived compound trigonelline (75% decrease) alongside an elevation in endogenous taurine (19% increase) and a 28% increase in N1-methyl-2-pyridone-5-carboxamide (2-PY). Metabolites related to neurotransmitter systems, including acetylcholine (26% decrease) and acetyl-*β*-methylcholine (19% decrease), exhibited reductions, alongside a significant decrease (59%) in pipecolic acid, an intermediate of lysine degradation. Alterations in carbohydrate metabolism associated with HFD included increased levels of the oligosaccharide *D*-raffinose (173% increase) and the pentose phosphate pathway intermediate sedoheptulose (59% increase). Additionally, HFD significantly disrupted carnitine homeostasis, evidenced by marked reductions in DL-carnitine (3% decrease), propionylcarnitine (31% decrease), and 3-dehydrocarnitine (6% decrease) (Supplementary Appendix B, Table B.3).

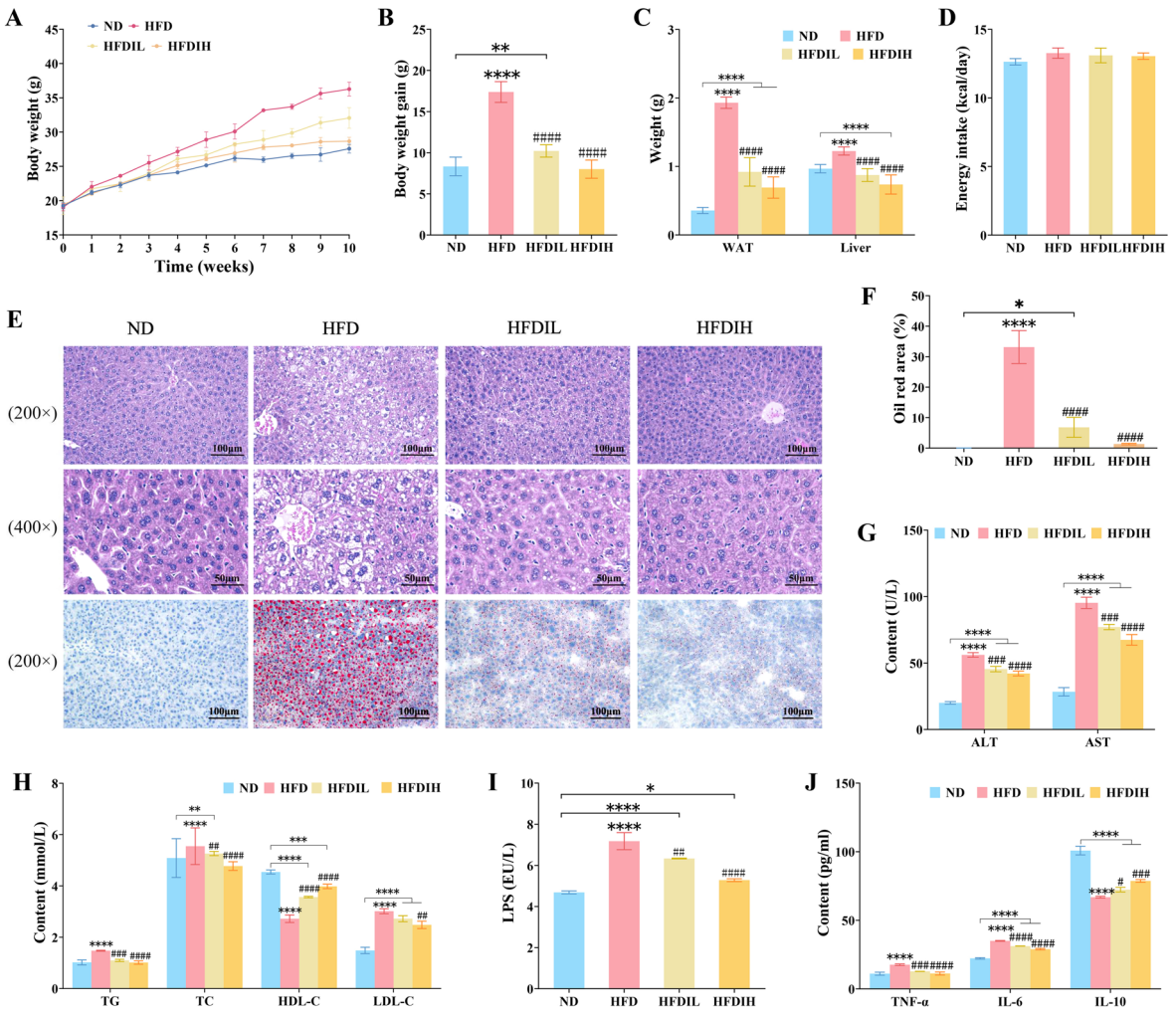

Fig. 3 Effects of *Isochrysis zhanjiangensis* on fat accumulation and serum indices. **A** Body weight. **B** Body weight gain. **C** White adipose tissue (WAT) mass and liver weight. **D** Energy intake. **E** Hepatic histopathology (H&E staining) and lipid droplets (Oil Red O staining). **F** Oil Red area. **G** Serum indices of alanine aminotransferase (ALT) and aspartate aminotransferase (AST). **H** Serum indices of triglycerides (TG), total cholesterol (TC), high-density lipoprotein cholesterol (HDL-C), and low-density lipoprotein cholesterol (LDL-C). **I** Lipopolysaccharide (LPS). **J** Tumor necrosis factor-alpha (TNF-α), interleukin-6 (IL-6), interleukin-10 (IL-10). $^{*}P<0.05$, $^{**}P<0.01$, $^{***}P<0.001$, $^{****}P<0.0001$ compared with ND; $^{\#}P<0.05$, $^{\#\#}P<0.01$, $^{\#\#\#}P<0.001$, $^{\#\#\#\#}P<0.0001$ compared with HFD

Supplementation with *I. zhanjiangensis* (HFDIH group) significantly modulated 19 metabolites compared to the HFD group, with nine metabolites partially or fully restored towards ND levels (Fig. 4D–L) (Supplementary Appendix B, Table B.4). For instance, the anti-inflammatory ω3 FA EPA, which HFD had depleted by 65% (relative to ND), increased by 146% in the HFDIH group (relative to HFD). Similarly, conjugated bile acids that were reduced by HFD (taurocholic acid: 60% decrease; cholic acid: 17% decrease, relative to ND) showed significant increases following intervention (taurocholic acid: 71% increase; cholic acid: 66% increase, relative to HFD). The plant-derived antioxidant trigonelline, suppressed by 75% under HFD (relative to ND), increased by 290% (relative to HFD), reaching near-normal levels. The HFD-induced accumulation of D-raffinose (173% increase relative to ND) was reversed, showing a 74% decrease in the HFDIH group (relative to HFD). Furthermore, acetyl-β-methylcholine, initially decreased by HFD (19%, relative to ND), increased significantly with supplementation (60%, relative to HFD). Additionally, a modest but significant decrease in hypotaurine (5%, relative to HFD) was observed. Furthermore, the intervention led to an increase in butyryl-L-carnitine levels (52%, relative to HFD), potentially counteracting some aspects of the HFD-induced carnitine dysregulation. Additionally, the NAD^{+}

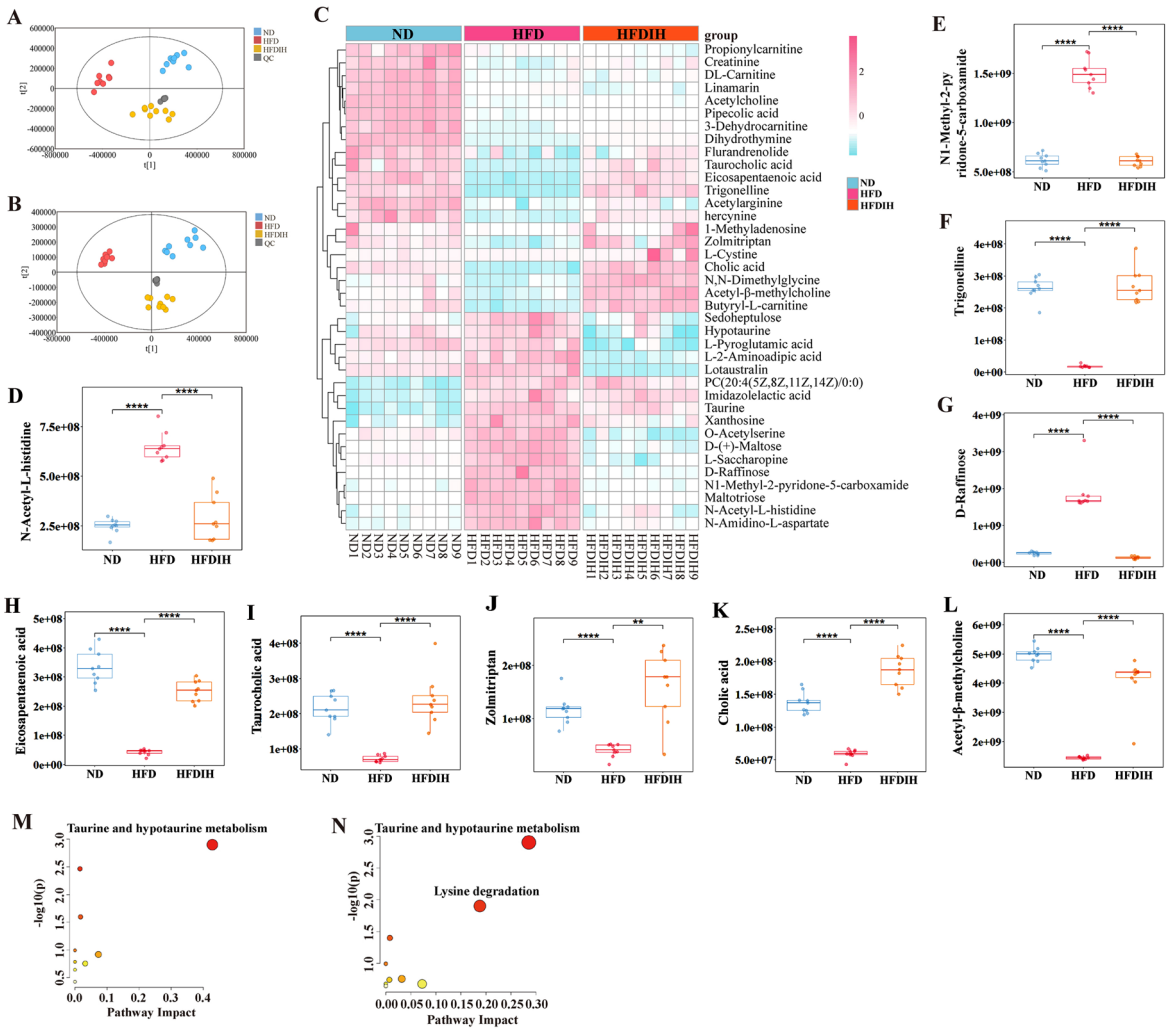

Fig. 4 Effects of *Isochrysis zhanjiangensis* on liver metabolic profile. The PCA score plots among all groups in (**A**) positive ion mode ($R^2X=0.776$, $Q^2=0.624$) and (**B**) negative ion mode ($R^2X=0.849$, $Q^2=0.664$). **C** The heatmap of all the differential metabolites. **D**–**L** The metabolites that were reversed after a HFD supplemented with *I. zhanjiangensis*. The pathway analysis (**M**) between ND and HFD groups and (**N**) between HFD and HFDIH groups ($n=9$). $^{**}P<0.01$, $^{****}P<0.0001$

catabolite 2-PY, which was elevated by HFD, showed a 22% decrease in the HFDIH group compared to HFD.

To understand broader metabolic impacts, KEGG pathway analysis was employed, comparing HFD versus ND (Fig. 4M) and HFDIH versus HFD (Fig. 4N). The analysis of HFD effects (Fig. 4M) highlighted taurine/hypotaurine metabolism as significantly disrupted, consistent with the observed increase in taurine and decrease in taurocholic acid. Supplementation with *I. zhanjiangensis* significantly modulated both taurine/hypotaurine metabolism and lysine degradation (Fig. 4N). Within the taurine/hypotaurine pathway, this modulation was reflected in the changes observed for hypotaurine and taurocholic acid, though not for taurine itself (as detailed previously). Regarding lysine degradation, while the HFD-induced decrease in pipecolic acid persisted post-intervention, pathway modulation by the supplement was confirmed through significant alterations in other measured intermediates within this pathway, namely L-2-aminoadipic acid (58% decrease vs. HFD) and L-saccharopine (29% decrease vs. HFD) (Supplementary Appendix B, Table B.4).

Effects of *I. zhanjiangensis* on gut microbiota diversity

Venn diagram analysis of microbial ASV distribution (Supplementary Appendix B, Fig. B.5A) revealed distinct patterns among ND, HFD, and HFDIH groups. The HFDIH group exhibited the highest number of unique ASVs (1467), followed by HFD (732) and ND (395). Pairwise overlaps

showed that HFDIH shared 225 ASVs with ND, 249 ASVs with HFD, while ND and HFD shared only 98 ASVs. A conserved core microbiome of 681 ASVs was shared across all three groups.

Alpha diversity analysis demonstrated progressive microbial community changes across dietary groups (Supplementary Appendix B, Fig. B.5B, C). The Chao1 index, reflecting species richness, increased from the ND group to HFD and reached the highest values in the HFDIH group, indicating that *I. zhanjiangensis* supplementation amplified HFD-induced microbial richness expansion. Similarly, the Shannon index, which integrates richness and evenness, showed a parallel trend: ND group maintained the lowest diversity, followed by HFD, with HFDIH exhibiting the most diverse community.

Principal coordinate analysis (PCoA) based on Bray–Curtis distances revealed significant spatial separation of gut microbiota communities among ND, HFD, and HFDIH groups (Supplementary Appendix B, Fig. B. 5D). The first two principal coordinates, PCoA1 (34.32% variance explained) and PCoA2 (12.82% variance explained), captured nearly half of the total microbial variation. The ND group formed a relatively compact cluster, reflecting a stable and conserved microbiota profile with minimal variation along PCoA1. However, it exhibited vertical dispersion along the positive PCoA2 axis, indicating some variability in community evenness. In contrast, the HFD group formed a distinct cluster in the right-central region, demonstrating significant divergence from ND and confirming a distinct microbiota profile induced by HFD. Notably, the HFDIH group formed a spatially segregated cluster adjacent to the HFD group in the lower-right quadrant, suggesting that *I. zhanjiangensis* supplementation altered the HFD-induced microbiota profile, positioning this group's profile between the ND and HFD clusters.

Impact of *I. zhanjiangensis* on gut microbiota phylogenetic restructuring

Taxonomic analysis at the phylum level revealed that gut microbiota in all groups were predominantly composed of Firmicutes and Bacteroidota (comprising over 90% of the relative abundance), with minor phyla including Proteobacteria, Actinobacteriota, and Verrucomicrobiota (Fig. 5A). Compared to the ND group, the HFD group exhibited a significant increase in Firmicutes and a concomitant decrease in Bacteroidota, resulting in an elevated Firmicutes/Bacteroidota (F/B) ratio from 0.25 to 2.41 (Fig. 5B–D). Notably, the HFDIH group showed partial restoration of this ratio to 1.82, indicating that *I. zhanjiangensis* intervention partially counteracted the HFD-induced shift in this ratio.

Phylogenetic analysis across multiple taxonomic levels revealed distinct shifts in microbial community composition among the dietary groups (Fig. 5E). The HFD group was predominantly enriched in members of Actinobacteria, Firmicutes, and Desulfobacterota, with expansions observed in sulfate-reducing Desulfovibrionaceae, obesity-associated Christensenellaceae, and inflammatory Enterobacteriaceae, alongside prominent clusters of Clostridiaceae and Lachnospiraceae. In contrast, the ND group was characterized by enrichment of fiber-fermenting families such as Mycoplasmataceae and Gastranaerophilales, with Bacteroidia and Vampirivibrionia forming the core of Bacteroidota in this sector. Radial branch thickness variations further highlighted HFD-driven enrichment of Coriobacteriaceae and Eggerthellaceae, whereas Tannerellaceae and Marinifilaceae occupied adjacent sectors predominantly enriched in the ND group. At the genus level, significant differences were also observed between the HFD and ND groups (Fig. 5F). The HFD group exhibited marked enrichment of genera linked to inflammation and metabolic dysregulation, including *Lachnospiraceae_FCS020_group*, *Escherichia-Shigella*, *Clostridium_sensu_stricto_1*, *UBA1819*, *Harryflintia*, *Intestinimonas*, *Peptococcus*, *Anaerotruncus*, *Parabacteroides*, *Rikenellaceae_RC9_gut_group*, *Enterorhabdus*, *Oscillibacter*, *Blautia*, and *Collinsella*. Sulfate-reducing genera related to Desulfovibrionaceae were also expanded in HFD samples. Conversely, the ND group was enriched in fiber-degrading and short-chain fatty acid (SCFA)-producing genera such as *Muribaculaceae*, *Mycoplasma*, *Prevotellaceae_NK3B3 1_group*, *Muribaculum*, *Clostridium_leptum*, *Gastranaerophilales*, *Vampirivibrio*, and *Parasutterella*. These genus-level differences reflected the pronounced impact of HFD on gut microbial community composition, consistent with shifts observed at higher taxonomic levels.

Microbial network analysis revealed substantial overlap between the HFD and HFDIH groups, yet intervention-specific modulations were apparent (Fig. 6A). Supplementation with *I. zhanjiangensis* significantly reduced HFD-associated pro-inflammatory Enterobacterales (phylum Proteobacteria) and mucin-degrading Coriobacteriales (phylum Actinobacteria), while enhancing Porphyromonadaceae (phylum Bacteroidota) and promoting proliferation of butyrate-producing Firmicutes lineages including Veillonellaceae, Selenomonadales, and Negativicutes. At the genus level (Fig. 6B), *I. zhanjiangensis* supplementation markedly increased the relative abundance of beneficial genera such as *Muribaculum*, *Candidatus_Arthromitus*, and *Veillonella*, taxa implicated in maintaining gut barrier integrity and SCFA production. In contrast, genera enriched in the HFD group without intervention included *Escherichia-Shigella*, *Alistipes_shahii*, and *Adlercreutzia_muris*, taxa previously associated with pro-inflammatory conditions.

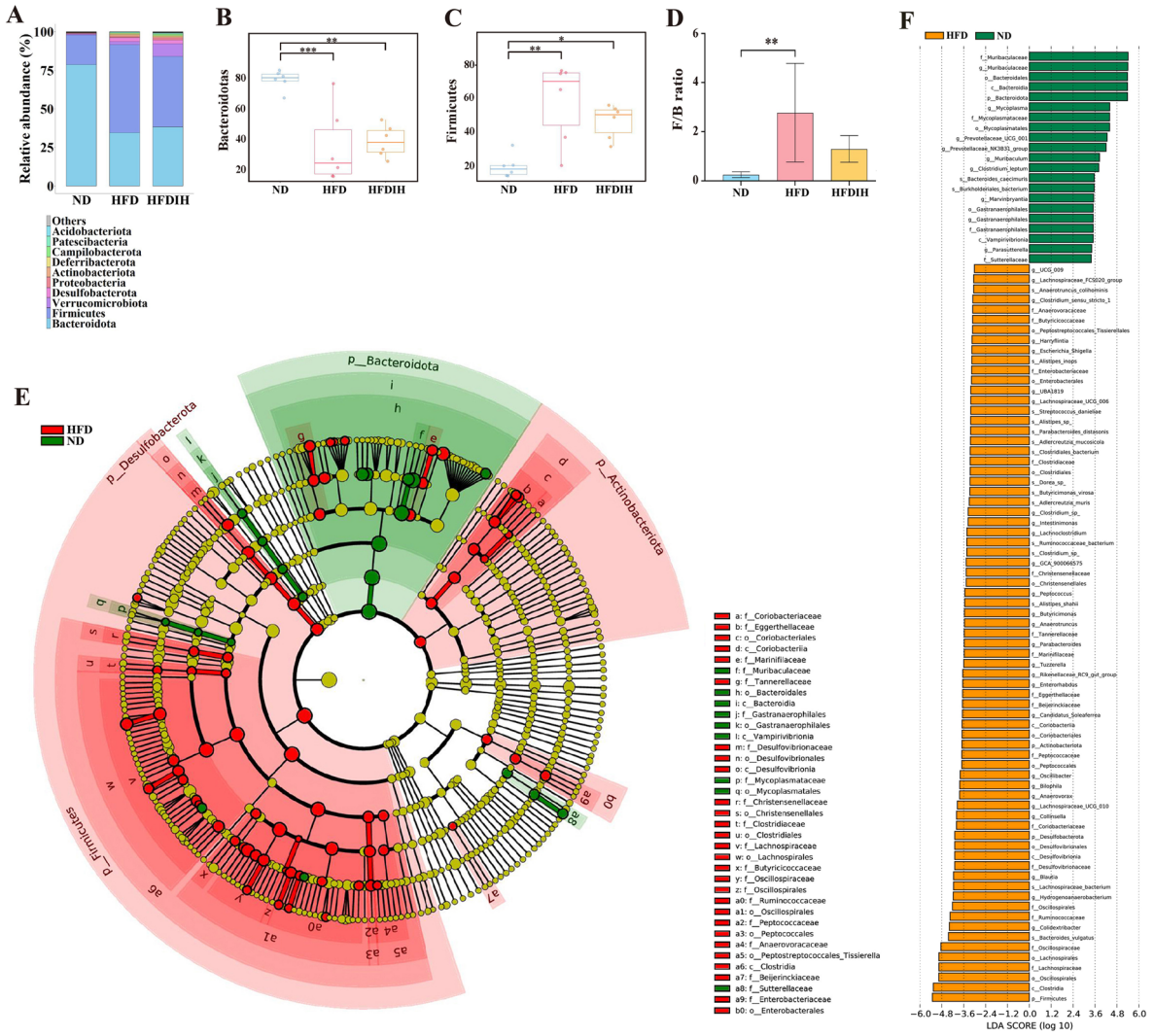

Fig. 5 Gut microbiota analysis ($n=6$). **A** Community composition at the phylum level among ND, HFD, and HFDIH. **B**–**D** Relative abundances of Firmicutes, Bacteroidota, and F/B ratio among different groups. **E** LEfSe cladograms illustrating differential bacterial taxa enriched in HFD (red) compared to ND (green). Rings from the center outward represent taxonomic levels from phylum to genus. Colored nodes indicate taxa with significant differences. **F** LDA scores showing significantly enriched bacterial taxa (LDA threshold > 3.0). Positive LDA scores (green bars) indicate taxa enriched in ND **F**, while negative scores (orange bars) indicate taxa enriched in HFD. $^{*}P<0.05$, $^{**}P<0.01$, $^{***}P<0.001$

Correlation analysis of gut microbiota, liver metabolites, and host phenotypic parameters

To explore the potential interplay between gut microbiota, liver metabolic alterations, and host physiological status, we further performed a correlation analysis integrating data on gut microbial relative abundances, liver metabolite levels, and various physiological and biochemical indices. The results were visualized using a correlation heatmap (Fig. 7A) and a focused correlation network (Fig. 7B).

The relative abundance of *Muribaculum* exhibited significant negative correlations with multiple biochemical parameters associated with obesity and inflammation, including BW, WAT, LDL-C, TC, ALT, AST, LPS, TNF-α, and IL-6. Conversely, *Muribaculum* showed positive correlations with HDL-C and IL-10.

A similar pattern of correlations was observed for the liver metabolite EPA, which demonstrated significant negative correlations with the aforementioned obesity-related markers, along with positive correlations with HDL-C and IL-10 (Fig. 7A). In contrast, several other liver metabolites,

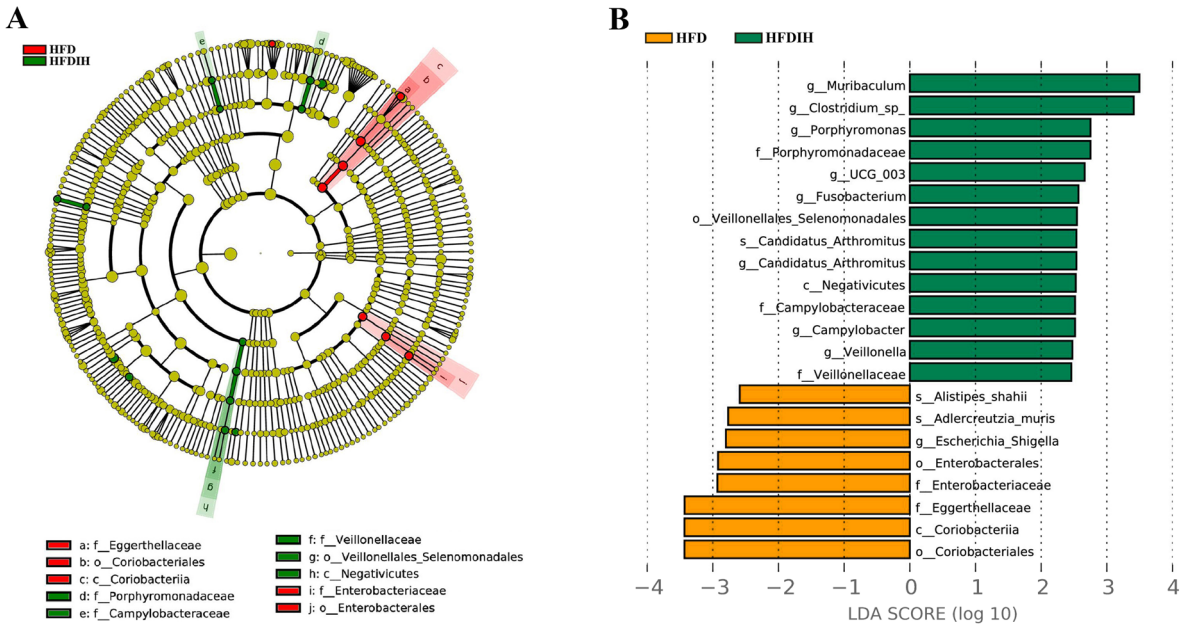

Fig. 6 Gut microbiota analysis comparing HFD and HFDIH groups ($n=6$). **A** LEfSe cladogram illustrating differential bacterial taxa enriched in HFD (red) compared to HFDIH (green). Rings from the center outward represent taxonomic levels from phylum to genus. Colored nodes indicate taxa with significant differences. **B** LDA scores showing significantly enriched bacterial taxa (LDA threshold > 3.0). Positive LDA scores (green bars) indicate taxa enriched in HFDIH, while negative scores (orange bars) indicate taxa enriched in HFD

including 2-PY and NAH, displayed significant positive correlations with markers such as BW, LDL-C, TC, ALT, AST, LPS, and IL-6.

Further insights were gained from the network analysis (Fig. 7B), which positioned *Muribaculum* and 2-PY as central nodes within the integrated microbial-metabolite-host interaction network. Their high degree of connectivity indicated they were associated with numerous microbial, metabolic, and physiological parameters measured in this study. Additionally, other metabolites, including EPA and NAH, also demonstrated multiple significant correlations with key biochemical parameters within this network.

Discussion

The nutritional characteristics of *I. zhanjiangensis*

In this study, comprehensive nutritional characterization confirmed that *I. zhanjiangensis* possesses a desirable profile as a potential functional food candidate. It exhibited a high lipid content accompanied by a moderate protein level, highlighting its potential as a valuable dietary source of lipids and proteins. Compared with microalgae such as *Chlorella vulgaris* and *Phaeodactylum tricornutum*, the relatively lower ash content in *I. zhanjiangensis*, attributable to the absence of a rigid cell wall, suggests enhanced digestibility and improved bioavailability of nutrients (Batista et al. 2019; Demarco et al. 2022; Fang et al. 2024).

FAs analysis further highlighted the nutritional advantages of *I. zhanjiangensis*, particularly its rich composition of PUFAs, accounting for approximately 45.06% of total FAs. Notably, ω3 PUFAs, such as DHA and ALA, were predominant, resulting in an exceptionally low ω6/ω3 ratio of 0.25, approximately 20-fold lower than the threshold (5:1) recommended by the European Nutritional Societies for promoting optimal health (Dawczynski et al. 2007). Given the well-established benefits of ω3 PUFAs in preventing CVDs, hypertension, and type II diabetes (Matos et al. 2017; Yang et al. 2023b), the abundant presence of these bioactive lipids underscores the significant therapeutic potential of *I. zhanjiangensis* for metabolic health.

The PUFA/SFA ratio is another widely recognized nutritional index for assessing the impact of dietary fat composition on cardiovascular health, as PUFAs have been demonstrated to reduce levels of LDL-C and total serum cholesterol, whereas SFAs are typically associated with increased cholesterol concentrations. Consequently, a higher PUFA/SFA ratio is generally considered more favorable for cardiovascular health (Chen and Liu 2020). Additionally,

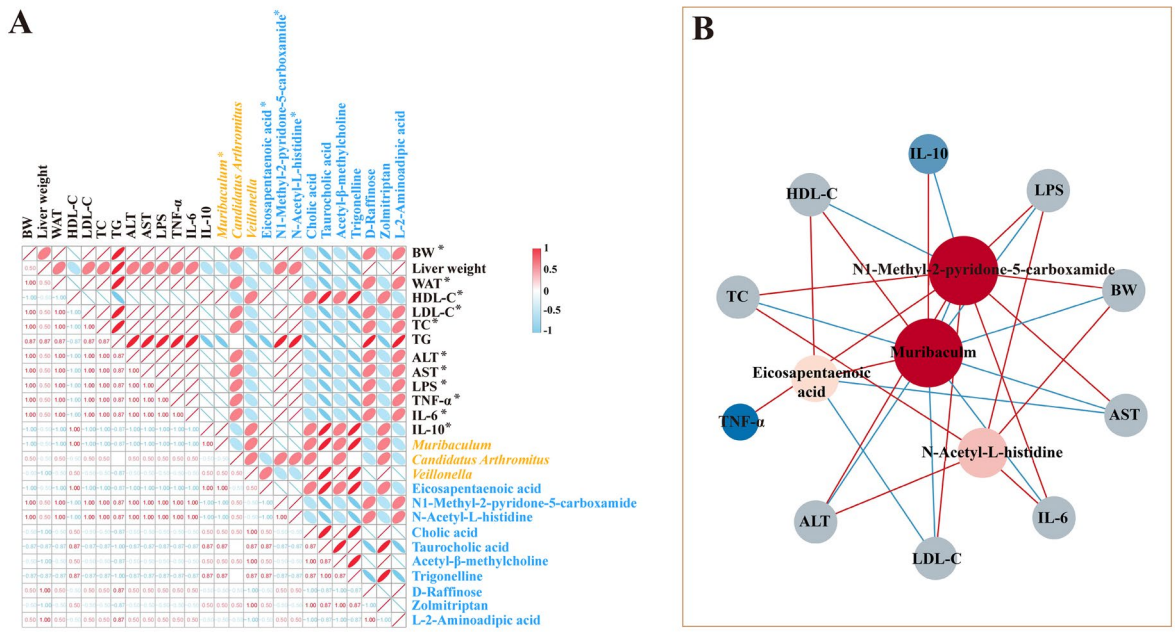

Fig. 7 The Spearman's correlation (**A**) heatmap and (**B**) network. The red and blue lines represent positive and negative correlations, respectively. BW: body weight; WAT: white adipose tissue mass; HDL-C: high-density lipoprotein cholesterol; LDL-C: low-density lipoprotein cholesterol; TC: total cholesterol; TG: triglycerides; ALT: alanine aminotransferase; AST: aspartate aminotransferase; LPS: lipopolysaccharide; TNF-α: tumor necrosis factor-alpha; IL-6: interleukin-6, IL-10: interleukin-10. $^{*}P < 0.05$

the AI and TI, reflecting the risks of atherogenesis and thrombosis, respectively, are critical indicators of dietary fat quality, with lower values indicating more favorable cardiovascular health effects (Chen and Liu 2020). The HH ratio is another key parameter for evaluating the beneficial impact of dietary fats on cholesterol metabolism, with higher values associated with better protection against cardiovascular and non-communicable diseases (Rincon-Cervera et al. 2020). When compared with common dietary sources such as edible seaweeds, fish, and meat, *I. zhanjiangensis* exhibited higher PUFA/SFA and HH ratios, along with lower AI and TI values, highlighting significant nutritional advantages and potential health benefits (Chen and Liu 2020; Kumar et al. 2010).

Regarding protein content, although the total protein level in *I. zhanjiangensis* is lower than in *Chlorella vulgaris* or *Nannochloropsis gaditana*, it remains comparable to *Haematococcus pluvialis* (Mularczyk et al. 2020; Ru et al. 2020). Importantly, its amino acid composition highlights its potential as a high-quality protein source, with 21 amino acids identified, including eight of the nine EAAs. The absence of tryptophan, likely due to extraction-induced degradation (Araya et al. 2021), suggests that the actual EAA profile of *I. zhanjiangensis* may align even more closely with the ideal protein standard. Furthermore, the calculated EAA/(EAA + NEAA) and EAA/NEAA ratios, at 35% and 54%, respectively, further underscore the nutritional quality of the protein content. Moreover, the presence of γ-aminobutyric acid, a NEAA known for neuroprotective and anti-anxiety effects, further enhances its potential as a functional food ingredient (Nikmaram et al. 2017).

Bioactive pigments in *I. zhanjiangensis*, particularly fucoxanthin and chlorophyll a, significantly contribute to its functional properties. Fucoxanthin, a carotenoid well-documented for its anti-obesity, antioxidant, and anti-inflammatory properties (Sun et al. 2023), is present at levels up to 15.6 mg/g in *I. zhanjiangensis*, which is tens to hundreds of times higher than those found in traditional edible seaweeds such as *Saccharina japonica*, *Hizikia fusiformis*, and *Undaria pinnatifida* (Leong et al. 2022). Similarly, the high chlorophyll a content further enhances the antioxidant potential of *I. zhanjiangensis*, as chlorophyll a has been demonstrated to effectively scavenge free radicals and provide protection against oxidative stress (Mendes et al. 2024).

The VOC profile of *I. zhanjiangensis*, dominated by acidic compounds, sulfur-containing derivatives, and halogenated hydrocarbons, exhibits significant divergence from traditional dietary sources. The prominence of carboxylic acids may impart pronounced acidic-pungent sensory characteristics, known to elicit sharp, vinegar-like notes even at trace concentrations due to their high volatility and low olfactory thresholds (Franklin and Mitchell 2019).

Concurrently, sulfur-containing volatiles introduce distinct sulfuraceous aromas reminiscent of alliaceous vegetables, rarely encountered in conventional protein sources (Park et al. 2024; Yu et al. 2022). Furthermore, halogenated hydrocarbons, such as chloroethene and fluorinated derivatives, contribute atypical ethereal and metallic undertones, deviating markedly from the alkane- and aldehyde-dominated profiles typical of marine organisms (Vilar et al. 2020). This unconventional combination of reactive functional groups results in a sensory profile distinctly different from the lipid oxidation-derived aldehydes or terpenoid-based volatiles commonly found in edible seaweeds (Vilar et al. 2020) and animal-derived foods (Zhao et al. 2025). While this chemical novelty presents opportunities for flavor innovation, the predominance of acidic and sulfurous compounds, coupled with halogenated hydrocarbons typically associated with industrial solvents, could challenge consumer acceptance thresholds. Strategic mitigation approaches, such as enzymatic neutralization of carboxylic acids or selective adsorption of halogenated compounds during processing (Xie et al. 2022), may reconcile the functional bioactivity of *I. zhanjiangensis* with sensory expectations, thus enhancing its viability as a novel functional food ingredient.

Safety assessment of *I. zhanjiangensis*

The rigorous toxicological evaluation conducted in this study clearly establishes *I. zhanjiangensis* as a safe dietary candidate. Acute toxicity testing revealed no signs of toxicity at the highest administered dose of 5000 mg/kg BW, equivalent to approximately 24.3 g/d for a 60 kg human based on body surface area normalization (Reagan-Shaw et al. 2008). This exposure exceeds typical human consumption of microalgae like *Spirulina* spp. and *Chlorella* spp. by an order of magnitude (Rzymski et al. 2018), indicating a considerable safety margin. These findings are consistent with safety evaluations of other aquaculture microalgae such as *Nannochloropsis* spp. and *Schizochytrium* spp. (Hammond et al. 2001; Kagan and Matulka 2015; Zanella and Vianello 2020).

Chronic administration studies further corroborated the safety profile and suggest dose-dependent beneficial metabolic effects rather than toxic effects. Specifically, mice receiving 400 mg/kg BW exhibited significant metabolic improvements, including reduction in BG and UA. These findings are consistent with previous studies demonstrating that *Chlorella vulgaris* intake improved insulin sensitivity and reduced BG levels in type 2 diabetic Goto-Kakizaki rats (Jeong et al. 2009), as well as with research showing that *Dunaliella salina* supplementation significantly decreased BG levels in streptozotocin-induced diabetic rats (El-Baz et al. 2020). These favorable metabolic responses can likely be attributed to bioactive compounds present in *I. zhanjiangensis*, such as fucoxanthin, known to enhance insulin sensitivity via AMP-activated protein kinase (AMPK) activation in hepatocytes (Ye et al. 2022), and potentially algal polyphenols inhibiting xanthine oxidase activity (Mehmood et al. 2022).

Notably, *I. zhanjiangensis* supplementation selectively elevated HDL-C levels by approximately 12% without significantly altering LDL-C or TG concentrations in this chronic safety study context. This lipid profile differs from interventions like oat β-glucan, which primarily lower LDL-C (Whitehead et al. 2014). The distinct HDL-C modulation observed might be partially attributed to the sterol composition of *I. zhanjiangensis*. Although not specifically characterized here, its close taxonomic relationship to *I. galbana* suggests the potential presence of sterols like brassicasterol and 24-methylenecholesterol (Iyad et al. 2016), known influencers of cholesterol metabolism (Cutignano et al. 2022; Volkman 2003). However, the precise mechanisms underlying this HDL-C-specific effect require further investigation to disentangle the contributions of sterols from other bioactive components.

Histopathological examinations further confirmed the safety of chronic dietary supplementation. Preserved hepatic architecture without evidence of microvesicular steatosis, a condition commonly reported in rodents fed certain microalgae (Velázquez et al. 2019), indicates effective lipid metabolism potentially facilitated by the high ω3 PUFA content of *I. zhanjiangensis*. Renal safety was affirmed by stable serum CRE concentrations and intact glomerular morphology, contrasting favorably with nephrotoxic cyanobacteria (Abeysiri et al. 2024; Yi et al. 2019).

Overall, these findings align well with the "Qualified Presumption of Safety" criteria proposed by EFSA for microalgae used in aquaculture (Koutsoumanis et al. 2023), significantly extending its potential extension to human nutrition. The demonstrated absence of adverse effects upon prolonged administration strongly endorses *I. zhanjiangensis* as a safe and novel functional food ingredient.

Alleviation of HFD-induced metabolic disorders by *I. zhanjiangensis*

Dietary supplementation with *I. zhanjiangensis* markedly mitigated HFD-induced metabolic disturbances, exerting concurrent beneficial effects on both systemic adiposity and hepatic health. A key finding was that both supplemented groups exhibited significantly reduced BW gain and adipose tissue accumulation despite comparable energy intake, strongly suggesting that the anti-obesity effect stems from enhanced metabolic efficiency or energy expenditure rather than appetite suppression. This aligns with the known bioactive components in *I. zhanjiangensis*, particularly fucoxanthin and ω3 PUFAs, which are recognized for stimulating

lipid catabolism and potentially thermogenesis, primarily in adipose tissue (Mayer et al. 2021).

Concomitantly, and likely sharing mechanistic underpinnings with the systemic anti-obesity effects, supplementation significantly improved hepatic health. This was evidenced by reduced lipid droplet accumulation, normalization of liver weight, and near-normalization of serum ALT and AST levels. While reduced systemic adiposity likely contributed indirectly by lessening hepatic lipid burden, bioactive components such as fucoxanthin and ω3 PUFAs are also known to directly modulate lipid metabolism within the liver. Specifically, they suppress de novo lipogenesis and enhance hepatic FA β-oxidation (Ha and Kim 2013; Mayer et al. 2021), thereby inhibiting intrahepatic lipid accumulation. Thus, *I. zhanjiangensis* coordinates multi-tissue lipid homeostasis through dual mechanisms: enhancing systemic energy expenditure while concurrently suppressing hepatic fat synthesis, ultimately contributing to the reversal of obesity-associated hepatosteatosis.

Beneficial effects also extended to systemic lipid metabolism, evidenced by improved serum lipid profiles: reductions in TG, TC, LDL-C, alongside elevated HDL-C. These lipid-normalizing effects could be attributed to ω3 PUFAs and potentially the phytosterols within *I. zhanjiangensis*, both classes of compounds possessing well-documented cholesterol-lowering properties (Lu et al. 2024; Micallef and Garg 2008). Consistent with this, studies on other ω3 PUFA-rich and phytosterol-containing microalgae demonstrate conserved mechanisms of lipid homeostasis enhancement, such as peroxisome proliferator-activated receptor-alpha (PPARα) activation and the suppression of very low-density lipoprotein secretion (Brosolo et al. 2023; Calder 2013; Kersten 2014; Manon et al. 2019).

Furthermore, *I. zhanjiangensis* exhibited potent anti-inflammatory effects, reversing HFD-induced elevations in pro-inflammatory mediators (TNF-α, IL-6) and LPS, and restoring anti-inflammatory IL-10 levels. These anti-inflammatory effects likely involve multiple pathways: ω3 PUFA competitively inhibiting pro-inflammatory prostanoid synthesis (Mayer et al. 2021), fucoxanthin suppressing NF-κB-mediated cytokine production (Martinez-Micaelo et al. 2012), and potentially improved gut barrier integrity as suggested by reduced circulating LPS, a marker of metabolic endotoxemia (Mayer et al. 2021). These findings align with previous reports demonstrating that the ability of microalgal components, including ω3 PUFA and carotenoids like fucoxanthin, to ameliorate HFD-induced inflammation (Banaszak et al. 2024; Sun et al. 2023).

Collectively, dietary supplementation with *I. zhanjiangensis* comprehensively ameliorated HFD-induced metabolic disorders, including obesity, hepatic steatosis, dyslipidemia, and systemic inflammation. These multi-target effects highlight its potential as a novel functional food for managing metabolic syndrome. The observed benefits likely arise from synergistic interactions among its bioactive components, including ω3 PUFAs, carotenoids, and potentially dietary fibers, acting through interconnected metabolic and immune pathways. Further characterization of its phytosterol and fiber contents and their specific contributions will be valuable in fully elucidating its therapeutic potential.

Metabolic modulation by *I. zhanjiangensis*

Hepatic metabolomics analysis revealed profound systemic dysregulation induced by HFD consumption and highlighted the multifaceted restorative effects of *I. zhanjiangensis* supplementation. The clear separation among ND, HFD, and HFDIH groups in PCA and OPLS-DA validated the significant metabolic perturbations caused by HFD. The intermediate metabolic profile of the HFDIH group indicated partial metabolic restoration, implying that *I. zhanjiangensis* mediates these effects through both direct biochemical modulation and indirect regulation of interconnected metabolic pathways.

Central to these beneficial effects was the reversal of key lipid mediators. The substantial recovery of EPA (146% increase in HFDIH vs. HFD), a critical ω3 PUFA depleted by HFD, is likely fundamental to the observed metabolic improvements. EPA serves as a precursor to specialized pro-resolving mediators, such as resolvins and protectins, which enhance anti-inflammatory signaling and promote lipid β-oxidation via PPARα activation (Calder 2013; Kersten 2014). These mechanisms align closely with the observed reductions in hepatic steatosis and systemic inflammation markers. Additionally, the notable restoration of taurocholic acid levels indicates improved bile acid metabolism. This enhancement likely improves lipid emulsification and activates farnesoid X receptor (FXR)-mediated pathways critical for regulating gluconeogenesis and lipogenesis (Chiang and Ferrell 2022; Zhang et al. 2006).

The beneficial effects of *I. zhanjiangensis* extended to pathways crucial for cellular energy metabolism and redox balance. HFD markedly increased the accumulation of the oligosaccharide D-Raffinose, an alteration significantly reversed by the intervention, suggesting improved carbohydrate handling. Concurrently, the plant-derived antioxidant Trigonelline, suppressed by HFD, was substantially restored by *I. zhanjiangensis* supplementation, likely contributing to an improved cellular redox state and counteracting HFD-induced oxidative stress. Furthermore, the intervention significantly impacted NAD^+ catabolism, evidenced by the marked decrease observed for 2-PY, a key NAD^+ breakdown product. This reduction in 2-PY levels may suggest altered NAD^+ turnover or flux, potentially indicating enhanced NAD^+ salvage or utilization efficiency (Holeček 2020; Pelantova et al. 2016), although further investigation

is needed to fully elucidate the impact on overall NAD^+ homeostasis. Collectively, the normalization of D-Raffinose, restoration of Trigonelline, and modulation of 2-PY point towards improved metabolic efficiency and redox control.

KEGG pathway analysis revealed that *I. zhanjiangensis* supplementation selectively modulated key metabolic pathways, rather than broadly normalizing all HFD-perturbed pathways. Within taurine/hypotaurine metabolism, while HFD-induced taurine elevation was not fully normalized (potentially reflecting persistent oxidative stress responses), the intervention actively modulated this pathway, evidenced by a significant decrease in hypotaurine levels. This suggests a specific interaction with this pathway, even if complete restoration of all metabolites was not achieved. Similarly, the lysine degradation pathway exhibited differential regulation. Although HFD-induced suppression of pipecolic acid remained refractory (possibly indicating persistent downstream enzymatic blocks or altered flux (Hallen et al. 2013)), *I. zhanjiangensis* significantly impacted upstream intermediates (*i.e.*, reductions in L-2-aminoadipic acid and L-saccharopine). This targeted downregulation of upstream intermediates may signify metabolic rerouting, potentially including enhanced carnitine biosynthesis, consistent with the observed normalization of butyryl-L-carnitine (52% increase vs. HFD). These KEGG findings highlight the nuanced and targeted nature of the microalgal metabolic effects, demonstrating precise, node-specific modulation within complex pathways, complementing its broader restorative actions on lipid and bile acid metabolism.

Collectively, these findings demonstrate that *I. zhanjiangensis* reprograms hepatic metabolism through synergistic mechanisms, prominently including ω3 PUFA-driven anti-inflammatory and lipid-oxidation signaling; and bile acid-mediated enhancement of lipid processing and nuclear receptor activation. These multifaceted effects effectively counteract primary HFD-induced metabolic disturbances, such as lipid accumulation and potentially insulin resistance, as well as secondary consequences like oxidative stress and inflammation.

Gut microbiota modulation by *I. zhanjiangensis*

A key mechanism underlying the protective effects of *I. zhanjiangensis* appears to be the restoration of gut microbiota homeostasis. HFD feeding is known to induce gut dysbiosis, often characterized by an expansion of Firmicutes at the expense of Bacteroidota, resulting in an elevated F/B ratio commonly associated with obesity (Ma et al. 2020b; Mizota et al. 2022; Yang et al. 2023a). Consistent with these reports, a dramatic increase in the F/B ratio was observed in this study. Dietary supplementation with *I. zhanjiangensis* partially restored this ratio to 1.82, suggesting mitigation of the HFD-induced phylum-level imbalance. Such rebalancing towards a profile more akin to the ND group is indicative of improved gut health, consistent with other algae-based interventions alleviating HFD-induced dysbiosis (Chen et al. 2023; Liu et al. 2024b). The ability of *I. zhanjiangensis* whole biomass to modulate gut microbial composition aligns with previous findings using its extracts (Wen et al. 2024), reinforcing its capacity to reshape the gut microbiome.

Beyond phylum-level changes, *I. zhanjiangensis* elicited specific taxonomic shifts associated with metabolic benefits. Importantly, the HFDIH group showed increased abundances of beneficial commensals such as *Muribaculum*, *Candidatus_Arthromitus*, and *Veillonella* (Liu et al. 2022). *Muribaculum* (family Muribaculaceae), a prominent fiber-degrader producing SCFAs, has been linked to leanness and improved metabolic profiles (Drolz et al. 2019; Huang et al. 2023). In our study, *Muribaculum* abundance negatively correlated with pathological markers (*e.g.*, BW, TNF-α, IL-6, LPS, liver injury enzymes) and positively correlated with anti-inflammatory IL-10 and HDL-C. This suggests *Muribaculum* may mediate some anti-obesity and anti-inflammatory effects, potentially through SCFA production improving host metabolism and immunity. Additionally, the marked increase in *Candidatus_Arthromitus* (segmented filamentous bacteria) suggests strengthened gut barrier immunity, as these commensals promote IgA production and balanced T-cell responses (Drolz et al. 2019; Romero et al. 2023; Vallianou et al. 2021), thereby fortifying intestinal integrity and preventing pathogen overgrowth. Similarly, the increased population of *Veillonella*, a lactate-utilizer producing propionate and acetate (Scheiman et al. 2019), may further contribute to a more favorable SCFA profile, supporting gut epithelial health and systemic homeostasis. Collectively, the expansion of these beneficial microbes suggests a probiotic-like effect of *I. zhanjiangensis*, fostering communities that produce anti-inflammatory metabolites and reinforce the gut barrier. Conversely, *I. zhanjiangensis* supplementation constrained the growth of deleterious bacteria promoted by HFD. Pathogenic taxa associated with inflammation and metabolic dysfunction, such as gram-negative Enterobacteriaceae (*e.g.*, *Escherichia-Shigella*) and pathobionts like *Alistipes_shahii* and *Adlercreutzia_muris*, were reduced in HFDIH group compared to HFD. Notably, decreases in Enterobacterales (phylum Proteobacteria) and mucin-degrading Coriobacteriales were observed. Overgrowth of such bacteria under HFD conditions can erode the gut mucus layer and elevate endotoxin release, exacerbating systemic inflammation (metabolic endotoxemia) (Wan et al. 2018). By suppressing these microbes, *I. zhanjiangensis* likely helps preserve intestinal barrier function and reduces circulating LPS, consistent with the improved inflammatory profile in the HFDIH group.

In summary, *I. zhanjiangensis* profoundly modulates the gut microbiome towards a health-associated state. It

counteracts HFD-induced dysbiosis by partially restoring phylum balance, selectively enriching beneficial taxa, and suppressing harmful ones. These changes appear functionally relevant: the enriched taxa are known to support gut barrier integrity and produce metabolites (*e.g.*, SCFAs) that combat inflammation, whereas the suppressed taxa include key drivers of endotoxemia and metabolic disturbance. Through this microbiota-mediated mechanism, *I. zhanjiangensis* likely interrupts the vicious cycle of diet-induced gut dysbiosis and host metabolic inflammation. The resultant stabilization of the gut ecosystem complements the direct metabolic effects of *I. zhanjiangensis*, ultimately leading to the alleviation of HFD-induced metabolic disorders. This gut microbiota modulation highlights an important facet of *I. zhanjiangensis* as a functional food, underscoring that the benefits of this microalga are partly conveyed by the microbiome.

Mechanisms underlying the protective effects of *I. zhanjiangensis* against HFD-induced metabolic disorders

The protective effects of *I. zhanjiangensis* against HFD-induced metabolic dysregulation appear to involve a synergistic interplay between gut microbiota remodeling and hepatic metabolic reprogramming. Our correlation analysis highlights *Muribaculum* and EPA as central nodes, suggesting at least two complementary pathways: (1) Microbiota-dependent signaling: The increased abundance of *Muribaculum* likely enhances SCFA production, which activates intestinal G protein-coupled receptor 43 (GPR43) signaling. This activation may suppress macrophage NLRP3 inflammasome activation and enhance glucagon-like peptide-1 secretion. Through these mechanisms, SCFA-GPR43 signaling collectively improves insulin sensitivity and modulates adipokine profiles (Koh et al. 2016). Additionally, the specialized capability of *Muribaculum* to degrade algal polysaccharides like chrysolaminarin might confer unique prebiotic effects distinct from terrestrial dietary fibers (Lagkouvardos et al. 2019; Zhu et al. 2024), potentially contributing to the observed anti-inflammatory efficacy. (2) EPA-mediated lipid homeostasis: The restoration of hepatic EPA levels enhances PPARα activity, stimulating FA oxidation pathways while concurrently suppressing lipogenic transcription factors like sterol regulatory element-binding protein-1c (Albracht-Schulte et al. 2019; Wang et al. 2020). This regulatory shift reduces hepatic triglyceride accumulation, thereby alleviating steatosis and systemic inflammation. Furthermore, increased conjugated bile acids (*e.g.*, taurocholic acid) suggest potential FXR activation, a mechanism known to suppress hepatic gluconeogenesis and stimulate energy expenditure (Chiang and Ferrell 2020; Fang et al. 2015).

Metabolomic biomarkers provided further insights into inflammatory pathways. Elevated 2-PY levels correlated with pro-inflammatory markers, reflecting impaired NAD^+ homeostasis linked to PARP-1 activation-driven NAD^+ depletion in obesity-associated inflammation (Szántó and Bai 2020). NAH, structurally related to histidine derivatives, positively correlated with obesity markers (BW, LDL-C, ALT, TNF-α) and was reduced by the intervention. This implicates histamine metabolism, a pathway linked to adipose inflammation (Wang et al. 2024), possibly modulated via suppression of histamine-producing *Escherichia-Shigella* or direct inhibition of histidine decarboxylase. However, the cellular origins (host vs. gut microbiota) and causal roles of these biomarkers require validation through isotope tracing and microbial genetic manipulation.

Collectively, *I. zhanjiangensis* orchestrates an integrated response linking microbial ecology (*e.g.*, Muribaculum enrichment) with host metabolic pathways (EPA signaling, bile acid homeostasis, and SCFA-GPR43 axis) to counteract HFD-induced metabolic syndrome. Future research should validate these mechanisms using pharmacological inhibitors (*e.g.*, PARP-1 antagonists), stable isotope tracing, and gnotobiotic models colonized with SCFA-producing consortia. Investigating dietary fibers, with a focus on algal polysaccharides such as chrysolaminarin and their prebiotic effects on *Muribaculum*, will elucidate structure–function relationships beyond whole biomass effects. Concurrently, processing techniques to modulate sensory profiles (VOC optimization) must be addressed for consumer-driven product development.

Conclusion

In conclusion, this study establishes *I. zhanjiangensis* as a novel, safe, and effective functional food against diet-induced metabolic dysregulation. Its unique capacity to synergistically modulate the gut-liver axis—enriching beneficial *Muribaculum*, restoring hepatic EPA, and improving bile acid metabolism—transcends single-target approaches. Chronic supplementation actively counteracted obesity, hepatosteatosis, and inflammation via this microbiota-metabolite interplay, distinguishing it from conventional interventions. As a sustainably cultivated marine resource, *I. zhanjiangensis* offers an eco-friendly strategy for metabolic health. Future work should validate causality using gnotobiotic models and advance human trials to harness its full potential.

Supplementary Information The online version contains supplementary material available at https://doi.org/10.1007/s42995-025-00320-x.

Acknowledgements This work was supported by the National Natural Science Foundation of China (No. 32570423), the Ningbo Science and Technology Project (No. 2024J176), the Key Program of Science and Technology Innovation in Ningbo (2023Z118), and the Zhejiang Provincial Natural Science Foundation of China (LY22C190001).

Author contributions MW: Methodology, investigation, data curation, visualization, writing – original draft. YB: Methodology, investigation, data curation. YL: Software, formal analysis. KC: Data curation, supervision. JL: Methodology, investigation. JL: Formal analysis, validation. CZ: Conceptualization, methodology, writing—review and editing. SNA: Supervision, writing—review and editing. LZ: Formal analysis, validation. XY: Conceptualization, supervision, formal analysis. JH: Funding acquisition, supervision, writing—review and editing, project administration.

Data availability The data that support the findings of this study are available from the corresponding author, upon reasonable request.

Declarations

Conflict of interest The authors declare that there are no conflicts of interest.

Animal and human rights statement This article does not contain any experiments with human participants conducted by the authors. All animal experiments followed the National Institutes of Health (NIH) Guide for the Care and Use of Laboratory Animals (NIH Publications No. 80–23, revised 1996). The animal experiment scheme of this study was approved by the Animal Care and Use Committee of Ningbo University (Approval No. SYXK-2019-0005, May 25, 2022).

References

Abeysiri HASN, Wanigasuriya JKP, Suresh TS, Beneragama DH, Manage PM (2024) Nephrotoxicity of cylindrospermopsin (CYN) and microcystin-LR (MC-LR) on mammalian kidney: Wistar rat as a model assessment. Nat Environ Pollut Technol 23:1761–1773

Albracht-Schulte K, Gonzalez S, Jackson A, Wilson S, Ramalingam L, Kalupahana NS, Moustaid-Moussa N (2019) Eicosapentaenoic acid improves hepatic metabolism and reduces inflammation independent of obesity in high-fat-fed mice and in HepG2 cells. Nutrients 11:599

Araya M, García S, Rengel J, Pizarro S, Álvarez G (2021) Determination of free and protein amino acid content in microalgae by HPLC-DAD with pre-column derivatization and pressure hydrolysis. Mar Chem 234:103999

Atalah E, Cruz CMH, Izquierdo MS, Rosenlund G, Caballero MJ, Valencia A, Robaina L (2007) Two microalgae *Crypthecodinium cohnii* and *Phaeodactylum tricornutum* as alternative source of essential fatty acids in starter feeds for seabream (*Sparus aurata*). Aquaculture 270:178–185

Banaszak M, Dobrzyńska M, Kawka A, Górna I, Woźniak D, Przysławski J, Drzymała-Czyż S (2024) Role of omega-3 fatty acids eicosapentaenoic (EPA) and docosahexaenoic (DHA) as modulatory and anti-inflammatory agents in noncommunicable diet-related diseases—reports from the last 10 years. Clin Nutr ESPEN 63:240–258

Batista AP, Niccolai A, Bursic I, Sousa I, Raymundo A, Rodolfi L, Biondi N, Tredici MR (2019) Microalgae as functional ingredients in savory food products: application to wheat crackers. Foods 8:611

Brosolo G, Da Porto A, Marcante S, Picci A, Capilupi F, Capilupi P, Bertin N, Vivarelli C, Bulfone L, Vacca A, Catena C, Sechi LA (2023) Omega-3 fatty acids in arterial hypertension: is there any good news? Int J Mol Sci 24:9520

Calder PC (2013) Omega-3 polyunsaturated fatty acids and inflammatory processes: nutrition or pharmacology? Br J Clin Pharmacol 75:645–662

Chamorro-Cevallos G, Garduno-Siciliano L, Barron BL, Madrigal-Bujaidar E, Cruz-Vega DE, Pages N (2008) Chemoprotective effect of *Spirulina* (*Arthrospira*) against cyclophosphamide-induced mutagenicity in mice. Food Chem Toxicol 46:567–574

Chen J, Liu H (2020) Nutritional indices for assessing fatty acids: a mini-review. Int J Mol Sci 21:5965

Chen MF, Zhang YY, Di He M, Li CY, Zhou CX, Hong PZ, Qian ZJ (2019) Antioxidant peptide purified from enzymatic hydrolysates of *Isochrysis zhanjiangensis* and its protective effect against ethanol induced oxidative stress of HepG2 cells. Biotechnol Bioprocess Eng 24:308–317

Chen J, Xiao Y, Li D, Zhang S, Wu Y, Zhang Q, Bai W (2023) New insights into the mechanisms of high-fat diet mediated gut microbiota in chronic diseases. iMeta 2:69

Cheng Z, Li N, Chen Z, Li K, Qiao D, Zhao S, Zhang B (2023) Ingesting retrograded rice (*Oryza sativa*) starch relieves high-fat diet induced hyperlipidemia in mice by altering intestinal bacteria. Food Chem 426:136540

Chiang JYL, Ferrell JM (2020) Bile acid receptors FXR and TGR5 signaling in fatty liver diseases and therapy. Am J Physiol-Gastrointest Liver Physiol 318:G554–G573

Chiang JYL, Ferrell JM (2022) Discovery of farnesoid X receptor and its role in bile acid metabolism. Mol Cell Endocrinol 548:111618

Cutignano A, Conte M, Tirino V, Del Vecchio V, De Angelis R, Nebbioso A, Altucci L, Romano G (2022) Cytotoxic potential of the marine diatom *Thalassiosira rotula*: insights into bioactivity of 24-methylene cholesterol. Mar Drugs 20:595

Dawczynski C, Schubert R, Jahreis G (2007) Amino acids, fatty acids, and dietary fibre in edible seaweed products. Food Chem 103:891–899

Demarco M, Oliveira de Moraes J, Matos ÂP, Derner RB, de Farias NF, Tribuzi G (2022) Digestibility, bioaccessibility and bioactivity of compounds from algae. Trends Food Sci Technol 121:114–128

Drolz A, Horvatits T, Rutter K, Landahl F, Roedl K, Meersseman P, Wilmer A, Kluwe J, Lohse AW, Kluge S, Trauner M, Fuhrmann V (2019) Lactate improves prediction of short-term mortality in critically ill patients with cirrhosis: a multinational study. Hepatology 69:258–269

El-Baz FK, Salama A, Salama RAA, Gabr M (2020) *Dunaliella salina* attenuates diabetic neuropathy induced by STZ in rats: involvement of thioredoxin. Biomed Res Int 2020:11

Fang S, Suh JM, Reilly SM, Yu E, Osborn O, Lackey D, Yoshihara E, Perino A, Jacinto S, Lukasheva Y, Atkins AR, Khvat A, Schnabl B, Yu RT, Brenner DA, Coulter S, Liddle C, Schoonjans K, Olefsky JM, Saltiel AR et al (2015) Intestinal FXR agonism promotes adipose tissue browning and reduces obesity and insulin resistance. Nat Med 21:159–165

Fang Y, Cai Y, Zhang Q, Ruan R, Zhou T (2024) Research status and prospects for bioactive compounds of *Chlorella* species: composition, extraction, production, and biosynthesis pathways. Process Saf Environ Prot 191:345–359

Franklin LM, Mitchell AE (2019) Review of the sensory and chemical characteristics of almond (*prunus dulcis*) flavor. J Agric Food Chem 67:2734–2735

Ha AW, Kim WK (2013) The effect of fucoxanthin rich power on the lipid metabolism in rats with a high fat diet. Nutr Res Pract 7:287

Hallen A, Jamie JF, Cooper AJ (2013) Lysine metabolism in mammalian brain: an update on the importance of recent discoveries. Amino Acids 45:1249–1272

Hammond BG, Mayhew DA, Holson JF, Nemec MD, Mast RW, Sander WJ (2001) Safety assessment of DHA-rich microalgae from *Schizochytrium* sp.: II. developmental toxicity evaluation in rats and rabbits. Regul Toxicol Pharm 33:205–217

Holeček M (2020) Histidine in health and disease: metabolism, physiological importance, and use as a supplement. Nutrients 12:848

Huang Y, Ying N, Zhao Q, Chen J, Teow S-Y, Dong W, Lin M, Jiang L, Zheng H (2023) Amelioration of obesity-related disorders in high-fat diet-fed mice following fecal microbiota transplantation from inulin-dosed mice. Molecules 28:3997

Iyad AH, Christopher CP, Robert JH (2016) Sterol composition of blue mussels fed algae and effluent diets from finfish culture. J Shellfish Res 35:429–434

Jacobs DR Jr, Tapsell LC (2007) Food, not nutrients, is the fundamental unit in nutrition. Nutr Rev 65:439–450

Jeong H, Kwon HJ, Kim MK (2009) Hypoglycemic effect of *Chlorella vulgaris* intake in type 2 diabetic Goto-Kakizaki and normal Wistar rats. Nutr Res Pract 3:23

Kagan ML, Matulka RA (2015) Safety assessment of the microalgae *Nannochloropsis oculata*. Toxicol Rep 2:617–623

Kersten S (2014) Integrated physiology and systems biology of PPARα. Mol Metab 3:354–371

Koh A, De Vadder F, Kovatcheva-Datchary P, Bäckhed F (2016) From dietary fiber to host physiology: short-chain fatty acids as key bacterial metabolites. Cell 165:1332–1345

Koutsoumanis K, Allende A, Álvarez-Ordóñez A, Bolton D, Bover-Cid S, Chemaly M, de Cesare A, Hilbert F, Lindqvist R, Nauta M, Peixe L, Ru G, Simmons M, Skandamis P, Suffredini E, Cocconcelli PS, Fernández Escámez PS, Maradona MP, Querol A, Sijtsma L et al (2023) Update of the list of qualified presumption of safety (QPS) recommended microorganisms intentionally added to food or feed as notified to EFSA. EFSA J 21:7988

Kumar M, Kumari P, Trivedi N, Shukla MK, Gupta V, Reddy CRK, Jha B (2010) Minerals, PUFAs and antioxidant properties of some tropical seaweeds from Saurashtra coast of India. J Appl Phycol 23:797–810

Lagkouvardos I, Lesker TR, Hitch TCA, Gálvez EJC, Smit N, Neuhaus K, Wang J, Baines JF, Abt B, Stecher B, Overmann J, Strowig T, Clavel T (2019) Sequence and cultivation study of *Muribaculaceae* reveals novel species, host preference, and functional potential of this yet undescribed family. Microbiome 7:28

Leong YK, Chen CY, Varjani S, Chang JS (2022) Producing fucoxanthin from algae—recent advances in cultivation strategies and downstream processing. Bioresour Technol 344:126170

Li W, Luo C, Huang Y, Zhan J, Lei J, Li N, Huang X, Luo H (2020) Evaluation of antifatigue and antioxidant activities of the marine microalgae *Isochrysis galbana* in mice. Food Sci Biotechnol 29:549–557

Liu X, Zhang Y, Li W, Zhang B, Yin J, Liuqi S, Wang J, Peng B, Wang S (2022) Fucoidan ameliorated dextran sulfate sodium-induced ulcerative colitis by modulating gut microbiota and bile acid metabolism. J Agric Food Chem 70:14864–14876

Liu Q, Lin L, Li H, Qian ZJ (2024a) Neuroprotection of truncated peptide IIAVE from *Isochrysis zhanjiangensis*: quantum chemical, molecular docking, and bioactivity studies. Molecules 29:692

Liu W, Wang J, Gao Q, Shen W, Weng P, Wu Z, Qin W, Liu Y (2024b) Combined analysis of gut microbiota and metabolomics in high-fat model mice fed with *Chlorella pyrenoidosa* peptides. J Funct Foods 121:106410

Lu X, Yang S, He Y, Zhao W, Nie M, Sun H (2024) Nutritional value and productivity potential of the marine microalgae *Nitzschia laevis*, *Phaeodactylum tricornutum* and *Isochrysis galbana*. Mar Drugs 22:386

Ma K, Bao Q, Wu Y, Chen S, Zhao S, Wu H, Fan J (2020a) Evaluation of microalgae as immunostimulants and recombinant vaccines for diseases prevention and control in aquaculture. Front Bioeng Biotechnol 8:590431

Ma L, Ni Y, Wang Z, Tu W, Ni L, Zhuge F, Zheng A, Hu L, Zhao Y, Zheng L, Fu Z (2020b) Spermidine improves gut barrier integrity and gut microbiota function in diet-induced obese mice. Gut Microbes 12:1–19

Magni P, Macchi C, Morlotti B, Sirtori CR, Ruscica M (2015) Risk identification and possible countermeasures for muscle adverse effects during statin therapy. Eur J Intern Med 26:82–88

Manon LG, Eric LF, Claire M, Virginie M, Dominique L-G, Benoît S, Lionel U (2019) Microalgal carotenoids and phytosterols regulate biochemical mechanisms involved in human health and disease prevention. Biochimie 167:106–118

Martinez-Micaelo N, González-Abuín N, Terra X, Richart C, Ardèvol A, Pinent M, Blay M (2012) Omega-3 docosahexaenoic acid and procyanidins inhibit cyclo-oxygenase activity and attenuate NF-κB activation through a p105/p50 regulatory mechanism in macrophage inflammation. Biochem J 441:653–663

Matos J, Cardoso C, Bandarra NM, Afonso C (2017) Microalgae as healthy ingredients for functional food: a review. Food Funct 8:2672–2685

Mayer C, Richard L, Côme M, Ulmann L, Nazih H, Chénais B, Ouguerram K, Mimouni V (2021) The marine microalga, *Tisochrysis lutea*, protects against metabolic disorders associated with metabolic syndrome and obesity. Nutrients 13:430

Mehmood A, Li J, Rehman AU, Kobun R, Llah IU, Khan I, Althobaiti F, Albogami S, Usman M, Alharthi F, Soliman MM, Yaqoob S, Awan KA, Zhao L, Zhao L (2022) Xanthine oxidase inhibitory study of eight structurally diverse phenolic compounds. Front Nutr 9:966557

Mendes AR, Spínola MP, Lordelo M, Prates JA (2024) Chemical compounds, bioactivities, and applications of *Chlorella vulgaris* in food, feed and medicine. Appl Sci 14:10810

Micallef MA, Garg ML (2008) The lipid-lowering effects of phytosterols and (*n*-3) polyunsaturated fatty acids are synergistic and complementary in hyperlipidemic men and women. J Nutr 138:1086–1090

Mizota T, Hishiki T, Shinoda M, Naito Y, Hirukawa K, Masugi Y, Itano O, Obara H, Kitago M, Yagi H, Abe Y, Matsubara K, Suematsu M, Kitagawa Y (2022) The hypotaurine-taurine pathway as an antioxidative mechanism in patients with acute liver failure. J Clin Biochem Nutr 70:54–63

Mohammad BE, Wan MWO (2017) Differential growth and biochemical composition of photoautotrophic and heterotrophic *Isochrysis maritima*: evaluation for use as aquaculture feed. J Appl Phycol 29:1159–1170

Mularczyk M, Michalak I, Marycz K (2020) Astaxanthin and other nutrients from *Haematococcus pluvialis*-multifunctional applications. Mar Drugs 18:459

Nayak SN, Aravind B, Malavalli SS, Sukanth BS, Poornima R, Bharati P, Hefferon K, Kole C, Puppala N (2021) Omics technologies to enhance plant based functional foods: an overview. Front Genet 12:742095

Nikmaram N, Dar BN, Roohinejad S, Koubaa M, Barba FJ, Greiner R, Johnson SK (2017) Recent advances in gamma-aminobutyric acid (GABA) properties in pulses: an overview. J Sci Food Agric 97:2681–2689

Park S, Kim HW, Joo Lee C, Kim Y, Sung J (2024) Profiles of volatile sulfur compounds in various vegetables consumed in Korea using HS-SPME-GC/MS technique. Front Nutr 11:1409008

Pelantova H, Buganova M, Holubova M, Sediva B, Zemenova J, Sykora D, Kavalkova P, Haluzik M, Zelezna B, Maletinska L, Kunes J, Kuzma M (2016) Urinary metabolomic profiling in mice with diet-induced obesity and type 2 diabetes mellitus after treatment

with metformin, vildagliptin and their combination. Mol Cell Endocrinol 15:88–100
Qian H, Chao X, Williams J, Fulte S, Li T, Yang L, Ding WX (2021) Autophagy in liver diseases: a review. Mol Aspects Med 82:100973
Reagan-Shaw S, Nihal M, Ahmad N (2008) Dose translation from animal to human studies revisited. FASEB J 22:659–661
Rincon-Cervera MA, Gonzalez-Barriga V, Romero J, Rojas R, Lopez-Arana S (2020) Quantification and distribution of omega-3 fatty acids in south Pacific fish and shellfish species. Foods 9:233
Romero J, Catalán N, Ramírez C, Miranda C, Oliva M, Flores H, Romero M, Rojas R (2023) High abundance of *Candidatus* arthromitus in intestinal microbiota of *Seriolella violacea* (palm ruff) under reared conditions. Fishes 8:109
Ru ITK, Sung YY, Jusoh M, Wahid MEA, Nagappan T (2020) *Chlorella vulgaris*: a perspective on its potential for combining high biomass with high value bioproducts. J Appl Phycol 1:2–11
Rzymski P, Budzulak J, Niedzielski P, Klimaszyk P, Proch J, Kozak L, Poniedziałek B (2018) Essential and toxic elements in commercial microalgal food supplements. J Appl Phycol 31:3567–3579
Sakamoto K, Butera MA, Zhou C, Maurizi G, Chen B, Ling L, Shawkat A, Patlolla L, Thakker K, Calle V, Morgan DA, Rahmouni K, Schwartz GJ, Tahiri A, Buettner C (2025) Overnutrition causes insulin resistance and metabolic disorder through increased sympathetic nervous system activity. Cell Metab 37:121-137.e6
Scheiman J, Luber JM, Chavkin TA, MacDonald T, Tung A, Pham LD, Wibowo MC, Wurth RC, Punthambaker S, Tierney BT, Yang Z, Hattab MW, Avila-Pacheco J, Clish CB, Lessard S, Church GM, Kostic AD (2019) Meta-omics analysis of elite athletes identifies a performance-enhancing microbe that functions via lactate metabolism. Nat Med 25:1104–1109
Schoeler M, Ellero-Simatos S, Birkner T, Mayneris-Perxachs J, Olsson L, Brolin H, Loeber U, Kraft JD, Polizzi A, Martí-Navas M, Puig J, Moschetta A, Montagner A, Gourdy P, Heymes C, Guillou H, Tremaroli V, Fernández-Real JM, Forslund SK, Burcelin R et al (2023) The interplay between dietary fatty acids and gut microbiota influences host metabolism and hepatic steatosis. Nat Commun 14:9250017
Shah MR, Lutzu GA, Alam A, Sarker P, Kabir Chowdhury MA, Parsaeimehr A, Liang Y, Daroch M (2018) Microalgae in aquafeeds for a sustainable aquaculture industry. J Appl Phycol 30:197–213
Sun H, Yang S, Zhao W, Kong Q, Zhu C, Fu X, Zhang F, Liu Z, Zhan Y, Mou H, He Y (2023) Fucoxanthin from marine microalgae: a promising bioactive compound for industrial production and food application. Crit Rev Food Sci Nutr 63:7996–8012
Szántó M, Bai P (2020) The role of ADP-ribose metabolism in metabolic regulation, adipose tissue differentiation, and metabolism. Genes Dev 34:321–340
Tilg H, Adolph TE, Trauner M (2022) Gut-liver axis: pathophysiological concepts and clinical implications. Cell Metab 34:1700–1718
Vallianou N, Dalamaga M, Stratigou T, Karampela I, Tsigalou C (2021) Do antibiotics cause obesity through long-term alterations in the gut microbiome? A review of current evidence. Curr Obes Rep 10:244–262
Velázquez KT, Enos RT, Bader JE, Sougiannis AT, Carson MS, Chatzistamou I, Carson JA, Nagarkatti PS, Nagarkatti M, Murphy EA (2019) Prolonged high-fat-diet feeding promotes non-alcoholic fatty liver disease and alters gut microbiota in mice. World J Hepatol 11:619–637
Vilar EG, O'Sullivan MG, Kerry JP, Kilcawley KN (2020) Volatile compounds of six species of edible seaweed: a review. Algal Res 45:101740
Vizcaíno AJ, Saéz MI, López G, Arizcun M, Abellán E, Martínez TF, Cerón-García MC, Alarcón FJ (2016) *Tetraselmis suecia* and *Tisochrysis lutea* meal as dietary ingredients for gilthead sea bream (*Sparus aurata L.*) fry. J Appl Phycol 28:2843–2855
Volkman J (2003) Sterols in microorganisms. Appl Microbiol Biotechnol 60:495–506
Wan X, Li T, Liu D, Chen Y, Liu Y, Liu B, Zhang H, Zhao C (2018) Effect of marine microalga *Chlorella pyrenoidosa* ethanol extract on lipid metabolism and gut microbiota composition in high-fat diet-fed rats. Mar Drugs 16:498
Wang Y, Nakajima T, Gonzalez FJ, Tanaka N (2020) Ppars as metabolic regulators in the liver: lessons from liver-specific PPAR-null mice. Int J Mol Sci 21:2061
Wang Y, Fang F, Liu X (2024) Targeting histamine in metabolic syndrome: insights and therapeutic potential. Life Sci 358:123172
Wen Y, Zhou Y, Tian L, He Y (2024) Ethanol extracts of *Isochrysis zhanjiangensis* alleviate acute alcoholic liver injury and modulate intestinal bacteria dysbiosis in mice. J Sci Food Agric 104:4354–4362
Whitehead A, Beck EJ, Tosh S, Wolever TMS (2014) Cholesterol-lowering effects of oat β-glucan: a meta-analysis of randomized controlled trials. Am J Clin Nutr 100:1413–1421
Xie Y, Lyu S, Zhang Y, Cai C (2022) Adsorption and degradation of volatile organic compounds by metal–organic frameworks (MOFs): a review. Materials 15:7727
Yang L, Wang Y, Li Z, Wu X, Mei J, Zheng G (2023a) Brain targeted peptide-functionalized chitosan nanoparticles for resveratrol delivery: impact on insulin resistance and gut microbiota in obesity-related Alzheimer's disease. Carbohydr Polym 15:120714
Yang Y, Xia Y, Zhang B, Li D, Yan J, Yang J, Sun J, Cao H, Wang Y, Zhang F (2023b) Effects of different n-6/n-3 polyunsaturated fatty acids ratios on lipid metabolism in patients with hyperlipidemia: a randomized controlled clinical trial. Front Nutr 1:1166702
Ye J, Zheng J, Tian X, Xu B, Yuan F, Wang B, Yang Z, Huang F (2022) Fucoxanthin attenuates free fatty acid-induced nonalcoholic fatty liver disease metabolism/oxidative stress/inflammation via the AMPK/Nrf2/TLR4 signaling pathway. Mar Drugs 20:225
Yi X, Xu S, Huang F, Wen C, Zheng S, Feng H, Guo J, Chen J, Feng X, Yang F (2019) Effects of chronic exposure to microcystin-LR on kidney in mice. Int J Environ Res Public Health 16:5030
Yu P, Yang Y, Sun J, Jia X, Zheng C, Zhou Q, Huang F (2022) Identification of volatile sulfur-containing compounds and the precursor of dimethyl sulfide in cold-pressed rapeseed oil by GC–SCD and UPLC–MS/MS. Food Chem 367:130741
Zanella L, Vianello F (2020) Microalgae of the genus *Nannochloropsis*: chemical composition and functional implications for human nutrition. J Funct Foods 68:103919
Zhang Y, Lee FY, Barrera G, Lee H, Vales C, Gonzalez FJ, Willson TM, Edwards PA (2006) Activation of the nuclear receptor FXR improves hyperglycemia and hyperlipidemia in diabetic mice. Proc Natl Acad Sci 103:1006–1011
Zhao M, Liu Z, Zhang W, Xia G, Li C, Rakariyatham K, Zhou D (2025) Advance in aldehydes derived from lipid oxidation: a review of the formation mechanism, attributable food thermal processing technology, analytical method and toxicological effect. Food Res Int 203:115811
Zheng JY, Tao NP, Gong J, Gu SQ, Xu CH (2015) Comparison of non-volatile taste-active compounds between the cooked meats of pre- and post-spawning Yangtze *Coilia ectenes*. Fish Sci 81:559–568
Zhou Y, Zhang J, Xu K, Zhang W, Chen F, Liu B, Guo B (2025) Fucoxanthin improves serum lipids, liver metabolism and gut microbiota in hyperlipidemia mice. Food Sci Hum Wellness 14:9250017

Zhu Y, Chen B, Zhang X, Akbar MT, Wu T, Zhang Y, Zhi L, Shen Q (2024) Exploration of the *Muribaculaceae* family in the gut microbiota: diversity, metabolism, and function. Nutrients 16:2660

Publisher's Note Springer Nature remains neutral with regard to jurisdictional claims in published maps and institutional affiliations.

Springer Nature or its licensor (e.g. a society or other partner) holds exclusive rights to this article under a publishing agreement with the author(s) or other rightsholder(s); author self-archiving of the accepted manuscript version of this article is solely governed by the terms of such publishing agreement and applicable law.